PNAS RESEARCH ARTICLE | DEVELOPMENTAL BIOLOGY

SOX9 and SOX10 control fluid homeostasis in the inner ear for hearing through independent and cooperative mechanisms

Irene Y. Y. Szeto[a], Daniel K. H. Chu[a,1], Peikai Chen[a,1,2], Ka Chi Chu[a,1], Tiffany Y. K. Au[a], Keith K. H. Leung[a], Yong-Heng Huang[b,c,3], Sarah L. Wynn[a], Angel C. Y. Mak[a,4], Ying-Shing Chan[a], Wood Yee Chan[d,5], Ralf Jauch[a,b,c], Bernd Fritzsch[e,f], Mai Har Sham[a,5], Robin Lovell-Badge[g], and Kathryn S. E. Cheah[a,6]

Edited by Stefan Mundlos, Max Planck Institute for Molecular Genetics, Berlin, Germany; received December 23, 2021; accepted September 10, 2022 by Editorial Board Member Denis Duboule

The in vivo mechanisms underlying dominant syndromes caused by mutations in SRY-Box Transcription Factor 9 (*SOX9*) and *SOX10* (*SOXE*) transcription factors, when they either are expressed alone or are coexpressed, are ill-defined. We created a mouse model for the campomelic dysplasia $SOX9^{Y440X}$ mutation, which truncates the transactivation domain but leaves DNA binding and dimerization intact. Here, we find that $SOX9^{Y440X}$ causes deafness via distinct mechanisms in the endolymphatic sac (ES)/duct and cochlea. By contrast, conditional heterozygous *Sox9*-null mice are normal. During the ES development of $Sox9^{Y440X/+}$ heterozygotes, *Sox10* and genes important for ionic homeostasis are downregulated, and there is developmental persistence of progenitors, resulting in fewer mature cells. *Sox10* heterozygous null mutants also display persistence of ES/duct progenitors. By contrast, SOX10 retains its expression in the early $Sox9^{Y440X/+}$ mutant cochlea. Later, in the postnatal stria vascularis, dominant interference by $SOX9^{Y440X}$ is implicated in impairing the normal cooperation of SOX9 and SOX10 in repressing the expression of the water channel Aquaporin 3, thereby contributing to endolymphatic hydrops. Our study shows that for a functioning endolymphatic system in the inner ear, SOX9 regulates *Sox10*, and depending on the cell type and target gene, it works either independently of or cooperatively with SOX10. $SOX9^{Y440X}$ can interfere with the activity of both SOXE factors, exerting effects that can be classified as haploinsufficient/hypomorphic or dominant negative depending on the cell/gene context. This model of disruption of transcription factor partnerships may be applicable to congenital deafness, which affects ∼0.3% of newborns, and other syndromic disorders.

SOXE transcription factors | inner ear endolymphatic system | haploinsufficiency | dominant negative | developmental syndrome

Significance

Impairment of the endolymphatic system is a common cause of deafness. Our study of a mouse model of campomelic dysplasia, a syndrome characterized in part by deafness of unknown etiology, reveals the roles of SOX9 and its relative SOX10 in maintaining a functioning endolymphatic system. Early in its development, these SOXE factors are critical for regulating the differentiation of progenitors and the expression of ion transporters and channels essential for ionic homeostasis. Later, they control the expression of *Aqp3*, a water/glycerol channel. The data provide a rich resource for the discovery of deafness genes. Since *SoxE* genes have many roles in development and in stem cells, the principles we have found could be applicable to tissue-specific effects in syndromes.

The SOXE (Sex-determining region Y [SRY]–related HMG-box, group E) transcription factors SOX9 and SOX10 are essential for the specification and differentiation of many progenitor cell (ProgC) types and for the development of several organs and tissues (1, 2). The expression patterns of the two genes can be distinct (e.g., cartilage) or overlapping (e.g., neural crest, nervous system, inner ear). Misexpression studies in mice suggest that SOXE genes can be partially redundant (3–5). SOX9 and SOX10 have redundant functions in oligodendrocyte precursors (5). SOX8, the third member of the SOXE group in the SRY-related transcription factor (SOX) family, is widely expressed, and although it is not essential for normal embryonic development, it has a role in adult Sertoli cell function (2, 6). SOX8 and SOX10 have also been shown to be partially redundant in oligodendrocyte development (2, 3, 7).

Mutations in *SOX9* and *SOX10* are dominant, causing several syndromes affecting different organ systems. In humans, heterozygous mutations in *SOX10* are associated with sensorineural hearing loss in Waardenburg–Shah syndrome (types II and IV; Online Mendelian Inheritance in Man [OMIM] 611584 and 613266), Kallmann syndrome (8), peripheral demyelinating neuropathy, and central dysmyelinating leukodystrophy (PCWH; OMIM 609136) (9, 10). Heterozygous mutations in *SOX9* result in campomelic dysplasia (CD), which is a syndrome characterized by skeletal dysmorphology, XY female sex reversal (OMIM 114290), abnormal development of the kidneys, central nervous system, and sensorineural deafness of unknown etiology (11–13).

Hearing and balance require a functioning sensory and endolymphatic system in the inner ear. The cochlea detects sound, and the vestibular organs detect linear acceleration and gravity. The different sensory organs and the endolymphatic sac (ES) of the endolymphatic system are specified at the otic vesicle stage (14, 15). During the development of the otic vesicle, the elaborate membranous labyrinthine system becomes filled with endolymph, a specialized extracellular fluid essential for sensory function. Dysfunction of this fluid

Author contributions: I.Y.Y.S. and K.S.E.C. designed research; I.Y.Y.S., D.K.H.C., K.C.C., T.Y.K.A., K.K.H.L., Y.-H.H., and S.L.W. performed research; M.H.S. contributed new reagents/analytic tools; I.Y.Y.S., D.K.H.C., P.C., K.C.C., T.Y.K.A., K.K.H.L., Y.-H.H., A.C.Y.M., Y.-S.C., W.Y.C., R.J., B.F., R.L.-B., and K.S.E.C. analyzed data; P.C., K.C.C., and K.K.H.L. prepared figures; R.J., B.F., and R.L.-B. interpreted data; Y.-S.C., W.Y.C., R.J., M.H.S., and K.S.E.C. supervised research; K.S.E.C. acquired funding; P.C., K.C.C., K.K.H.L., R.J., B.F., and R.L.-B. edited the manuscript; and I.Y.Y.S. and K.S.E.C. wrote the paper.

The authors declare no competing interest.

This article is a PNAS Direct Submission. S.M. is a guest editor invited by the Editorial Board.

This article contains supporting information online at http://www.pnas.org/lookup/suppl/doi:10.1073/pnas.2122121119/-/DCSupplemental.

Published November 7, 2022.

pathway results in endolymphatic hydrops that causes hearing loss, vertigo, tinnitus, aural fullness, and pain. The ES is the first structure of the inner ear to develop and control endolymph volume and pressure (16). The stria vascularis on the lateral wall of the cochlear duct develops later, matures postnatally (postnatal day 3), generates the endocochlear potential between the endolymph and the perilymph, and regulates the ionic content of the endolymph. In a fully developed inner ear, endolymph secreted from the cochlear duct drains into the saccule and enters the endolymphatic duct (ED) and ES, where it is reabsorbed by the vascular system (17).

The roles of SOXE factors in the development of the endolymphatic system are not well defined. SOX9 and SOX10 are both expressed in the developing inner ear (18–20). *Sox9* is required for specification of otic placode (21) and essential for maintaining otic progenitors in *Xenopus* (22). It is widely expressed in the mouse inner ear during development (19, 22) and is required for otic invagination (18). Loss of *Sox9* expression in the periotic mesenchyme affects both otic capsule differentiation and cochlear coiling (23). Complete loss of *Sox10* in mice results in shortened cochlea ducts in both heterozygotes and homozygotes, which are attributed to the loss of cochlea progenitors, although those remaining are correctly differentiated (20). Although *Sox8* acts redundantly with *Sox9* in testes development, this may not be the case in the ear. In chicks, *Sox8* regulates *Sox10* in the otic vesicle, but this is not conserved in mice (24, 25). *Sox8* is expressed in the supporting cells in the sensory epithelium of the cochlea, but *Sox8*-null mice do not have inner ear defects (20, 26–28), suggesting a nonessential role in hearing.

CD is attributed to haploinsufficiency for SOX9 because there is no obvious correlation between the type or position of mutation and disease severity, a concept supported by the recapitulation of the cartilage defects in *Sox9* heterozygous null mutant mice (29). However, not all *SOX9* mutations result in the absence of protein. For example, some mutations in *SOX9* result in a truncated transactivation domain but intact DNA binding domain. Mechanisms, such as dominant negative effects, cannot be ruled out. There is no systematic or definitive comparison between probands affected by different *SOX9* mutations in terms of survival (30, 31). CD is usually described as "perinatal lethal," with some probands surviving to 2 y. However, some probands with the SOX9 Y440X mutation, which truncates the C-terminal transactivation domain, survive for up to 4 to 9 y (32–34). Intriguingly, residual transactivation activity of $SOX9^{Y440X}$ was demonstrated in vitro (13, 32–34), raising the possibility of a hypomorphic mechanism that allows for longer survival. By contrast, in vitro tests of other *SOX9* mutants with truncated C termini suggest a dominant negative effect (35).

In vitro assays show that SOX9 and SOX10 interact with each other and form homodimers as well as heterodimers (2, 36). SOXE factors also work with partner factors to regulate gene expression (37, 38). Important questions regarding disease mechanisms underlying heterozygosity for *SOXE* factors are how the mutation in one allele impacts the function of the normal allele or other coexpressed partners, leading to disease phenotypes. How heterozygous mutations in *SOX9* cause sensorineural deafness in CD and whether these impact the function of SOX10, its SOXE partner, are unknown.

To address these questions, we focused on delineating the molecular mechanism(s) underlying the least understood clinical aspect of CD caused by the $SOX9^{Y440X}$ mutation: sensorineural deafness. By comparing the impact on inner ear development of constitutive and otic-specific expression of the $SOX9^{Y440X}$ mutation in heterozygotes and heterozygous otic-specific *Sox9*-null and heterozygous *Sox10*-null mutants, we implicate essential roles for both SOXE factors in hearing and vestibular function. Early in inner ear development, both SOX9 and SOX10 control ProgC differentiation and ionic homeostasis for a functioning endolymphatic system of the inner ear. The SOXE factors also act cooperatively later in inner ear development, contributing to the functional properties of the stria vascularis in the cochlea, for example, by controlling the expression of a water/glycerol channel aquaporin 3 (AQP3). Overall, the developmental stage and inner ear cell-type context-dependent impact of the $SOX9^{Y440X}$ mutation combined with the disruption of the SOXE gene regulatory network leads to auditory and vestibular dysfunction.

Results

$Sox9^{Y440X}$ Causes Vestibular Dysfunction and Lack of Endocochlear Potential. To investigate the underlying basis for deafness in CD, we generated mice carrying a conditional targeted allele ($Sox9^{Y440X\text{-}IRES\text{-}EGFP}$; abbreviated $Sox9^{Y440X}$) comprising *Sox9* exon 3 flanked by loxP sites and a mutated exon 3 containing $Sox9^{Y440X}$ linked to an internal ribosome entry site–enhanced green fluorescent protein (IRES-EGFP) reporter, inserted downstream (Fig. 1*A* and *SI Appendix*, Fig. S1 *A–G*). Mice with the conditional allele were phenotypically and behaviorally normal and fertile. *Sox9* is expressed in the developing otic epithelium from embryonic day 8.5 (E8.5), the surrounding mesenchyme from E10.5, and the otic capsule at later stages (19, 23). Expression of the mutant allele, reported by GFP expression, was confirmed in the heterozygous embryos carrying an ubiquitously expressed β-actin Cre recombinase (cre)–directed knock-in allele of $Sox9^{Y440X}$. GFP expression recapitulates the endogenous pattern of *Sox9* in the otic vesicle at E10.5 and ES/ED and cochlea at E14.5 (*SI Appendix*, Fig. S1 *C–G*). We confirmed the specific and stable expression of truncated $SOX9^{Y440X}$ protein in the developing mutant ES/ED and cochlea using an antibody that recognizes the mutant protein specifically (Fig. 1 *B* and *C*). Approximately 10% of ubiquitous cre-induced constitutive $Sox9^{Y440X/+}$ mice survived, from which a heterozygous mutant line was established. No $Sox9^{Y440X/Y440X}$ homozygotes survived to birth. In addition to the skeletal phenotype typical of CD in newborns (*SI Appendix*, Fig. S1*B*), the surviving heterozygous mutant mice had kinked tails, showed circling behavior, and failed swimming tests, typical of vestibular disorders (Movies S1 and S2).

We generated conditional mutants ($B2\text{-}Sox9^{cY440X/+}$) using the HoxB2(r4)-Cre (*B2-r4-cre*) mouse that expresses CRE in the otic placode from E8.5 (39) to assess the effect of $Sox9^{Y440X}$ on inner ear development. Otic vesicles of E9.5 $B2\text{-}Sox9^{cY440X/+}$ embryos were morphologically normal. However, before weaning, mutants developed vestibular and auditory phenotypes, such as hyperactivity, head tossing and circling behavior (Movie S3), and head tilting (*SI Appendix*, Fig. S1*H*). They failed tests for reaching response (Fig. 1*D* and *SI Appendix*, Fig. S1*I*), contact righting, and negative geotaxis (Fig. 1 *E* and *F* and Movies S4 and S5). Their auditory brain stem responses showed a hearing deficit of 40 to 80 dB (Fig. 1*G* and *SI Appendix*, Fig. S1*J*), and the endocochlear potential was reduced to 2 mV in mature mutants (Fig. 1*H*).

Otic Expression of $Sox9^{Y440X}$ Causes Endolymphatic Hydrops. Endolymphatic hydrops is caused by disruption of endolymph homeostasis. Histology revealed endolymphatic hydrops in $B2\text{-}Sox9^{cY440X/+}$ mice (Fig. 1 *I*, *J*, and *L–U*). In adult mutants,

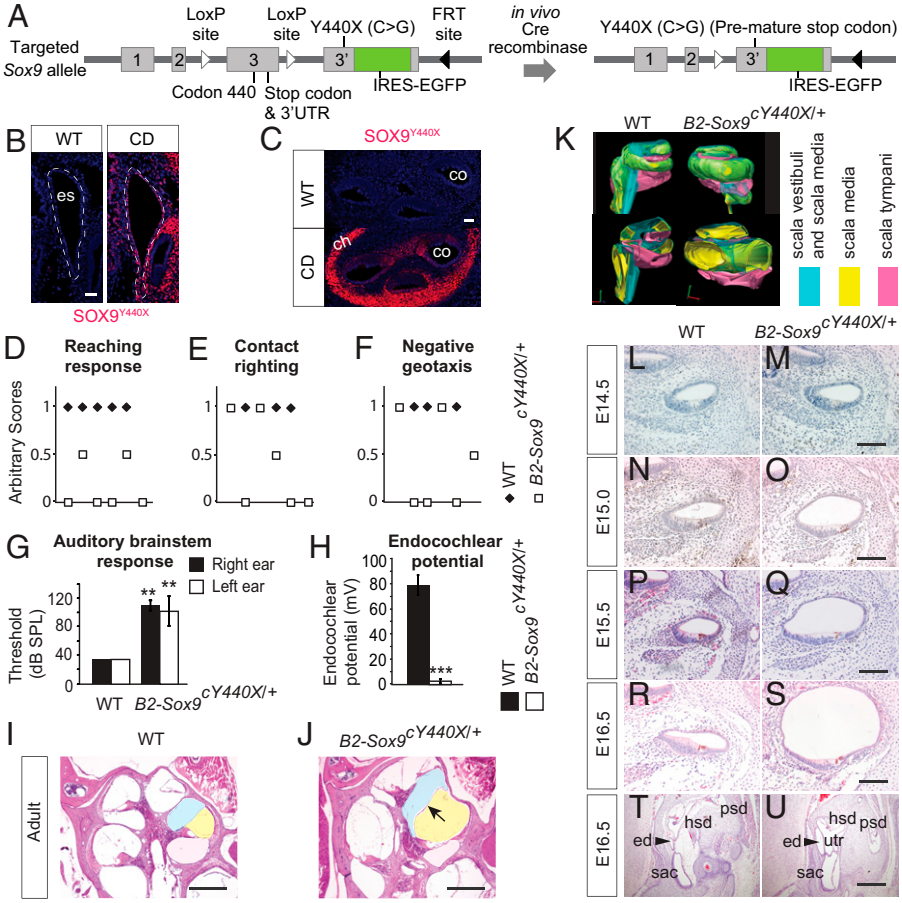

Fig. 1. Impaired vestibular and auditory function in *B2-Sox9*$^{cY440X/+}$ mutants. (*A*) Schematic diagram of the *Sox9*$^{cY440X/+}$ targeted allele comprising exon 3 flanked by LoxP sites followed by exon 3′ carrying the *Y440X* mutation and *IRES-EGFP* sequences. FRT, flippase recognition target. UTR, untranslated region. (*B* and *C*) Immunostaining of SOX9^{Y440X} in WT and *Sox9*$^{Y440X/+}$ (CD) ES (*B*) and cochlea (*C*) at E14.5 (n = 2). (*D*–*F*) *B2-Sox9*$^{cY440X/+}$ mutants displayed impaired vestibular function. (*D*) Reaching response: forelimbs stretched scored 1, curled ventrally scored 0, and curled slightly scored 0.5. (*E*) Contact righting: flipped back to upright position within 5 s scored 1, crawled upside down scored 0, and crawled sideways scored 0.5. (*F*) Negative geotaxis: turned and moved up the slope surface scored 1, failed to stay on the slope surface scored 0, and failed to turn and stayed scored 0.5 (WT n = 5; *B2-Sox9*^{cY440X} n = 6). (*G*) Thresholds for auditory brain stem response (sound pressure level [SPL]); 120-dB SPL was the highest level measured (n = 5). (*H*) Endocochlear potential in 4- to 7-mo-old WT and *B2-Sox9*$^{cY440X/+}$ mice (n = 4). (*I* and *J*) Cochlear ducts from WT (*I*) and *B2-Sox9*$^{cY440X/+}$ (*J*) adult animals at 6 mo. (*K*) Three-dimensional reconstruction of WT and *B2-Sox9*$^{cY440X/+}$ adult cochlea. Scala vestibule/scala media, scala media, and scala tympani are in blue, yellow, and pink, respectively. (*L*–*S*) Cochlear ducts from WT and *B2-Sox9*$^{cY440X/+}$ embryos at E14.5 (*L* and *M*), E15.0 (*N* and *O*), E15.5 (*P* and *Q*), and E16.5 (*R* and *S*; n = 2 to 4). (*T* and *U*) Transverse sections of WT and *B2-Sox9*$^{cY440X/+}$ ED (ed; arrowhead) at E16.5 (n = 2). Data are presented as means ± SEM. Results for the CD mutants are from the constitutively active *Sox9*$^{Y440X/+}$ samples unless labeled as conditional. ch, chondrocyte; co, cochlea; es, ES; hsd, horizontal semicircular duct; psd, posterior semicircular duct; sac, saccule; utr, utricle. (Scale bars: 40 μm in *B* and *C*; 100 μm in *M*, *O*, *Q*, and *S*; 400 μm in *I*, *J*, and *U*.) $^{**}P < 0.01$; $^{***}P < 0.001$.

the scala media containing the endolymph were expanded, with a distended Reissner's membrane (Fig. 1 *I* and *J*). Reconstruction of the cochlea structure in three dimensions (Fig. 1*K* and *SI Appendix*, Fig. S1*K*) showed that of the three sound-conducting chambers, the scala media in the mutant were twice the volume of that in the wild type (WT), while the scala tympani was one-third smaller; the scala vestibuli were of the same size. Consistent with volume changes in the developing ear (40), expansion of the cochlear duct was not detectable at E14.5 (Fig. 1 *L* and *M*), but it was apparent by E15.0 (Fig. 1 *N* and *O*) and became more prominent and obvious at E16.5 (Fig. 1 *R* and *S*) and in adults (Fig. 1 *I* and *J*). At P9, we found otoconia deficiency in the mutant utricle and saccule, an indication of defects in the endolymphatic system (*SI Appendix*, Fig. S1*L*). Scanning electron microcopy of the inner ears of *B2-Sox9*$^{cY440X/+}$ mice at P4 showed normal arrangement of hair cells and stereocilia in the organ of Corti, suggesting that the hearing deficit is not caused by abnormal prosensory development (*SI Appendix*, Fig. S1*M*). Assessment of the relative numbers of bromodeoxyuridine (BrdU)–labeled proliferating cells (ProlCs) and terminal deoxynucleotidyl transferase dUTP nick end labeling (TUNEL)–positive apoptotic cells among the total number of cochlea epithelial cells at E14.5 showed no significant differences between WT and mutants (*SI Appendix*, Fig. S1 *N*–*S*), suggesting that cell proliferation and survival were not affected.

Fewer *Slc26a4*-Expressing Cells in the *Sox9*$^{Y440X/+}$ Mutant ES. The mouse *Lmx1a* functional null mutant *dreher* (drJ/drJ) (41–43) lacks an ED, while patients with LMX1A mutations have impaired hearing (44, 45). Normal *Lmx1a* expression in the prospective ES of the *Sox9*$^{Y440X/+}$ mutants at E10.5 indicates proper specification of the rudiment (*SI Appendix*, Fig. S1 *T*). The ED was enlarged in *B2-Sox9*$^{cY440X/+}$ mutants at E16.5 compared with WT (Fig. 1 *T* and *U*), reminiscent of hydropic ears (46). In humans, enlarged ES and cochlea are characteristic of Pendred syndrome caused by homozygous mutations in *SLC26A4* (Pendrin) encoding an anion exchanger (47, 48); heterozygous mutations in the transcription factor *FOXI1* (OMIM 601093), which activates *SLC26A4* transcription (49); or compound heterozygous mutations for both *SLC26A4* and *FOXI1*. In mice, disruption of NaCl resorption mediated by FOXI1 and its target *Slc26a4* causes enlargement of the endolymphatic compartment, endolymph imbalance, and deafness (50). Mice lacking SLC26A4 in the ES develop endolymphatic hydrops (51). We examined if *Sox9*$^{Y440X/+}$ impacts on *Slc26a4* expression. The signal intensity of in situ hybridization for *Slc26a4* in the mutant ES appeared unchanged, but the preponderance of *Slc26a4*-expressing cells was significantly reduced by 40% (Fig. 2 *A* and *B*), which may contribute to the deafness phenotype.

Immature and Mature Cell Populations Are Present in the *Sox9*$^{Y440X/+}$ ES. The reduced proportion of *Slc26a4*-expressing cells in the ES could arise from an effect of *Sox9*^{Y440X} on the activation of gene expression and/or cell identity. To examine both possibilities, we sequenced the transcriptomes of single cells isolated from WT (91 cells, n = 3) and *Sox9*$^{Y440X/+}$ (155 cells, n = 2) ESs at E14.5 before an apparent phenotype. Using principal component analysis (52), we identified three cell populations and defined cluster-specific signatures by determining the differentially expressed genes (DEGs) of each cluster vs. all other clusters (Dataset S1) and by reference to single-cell

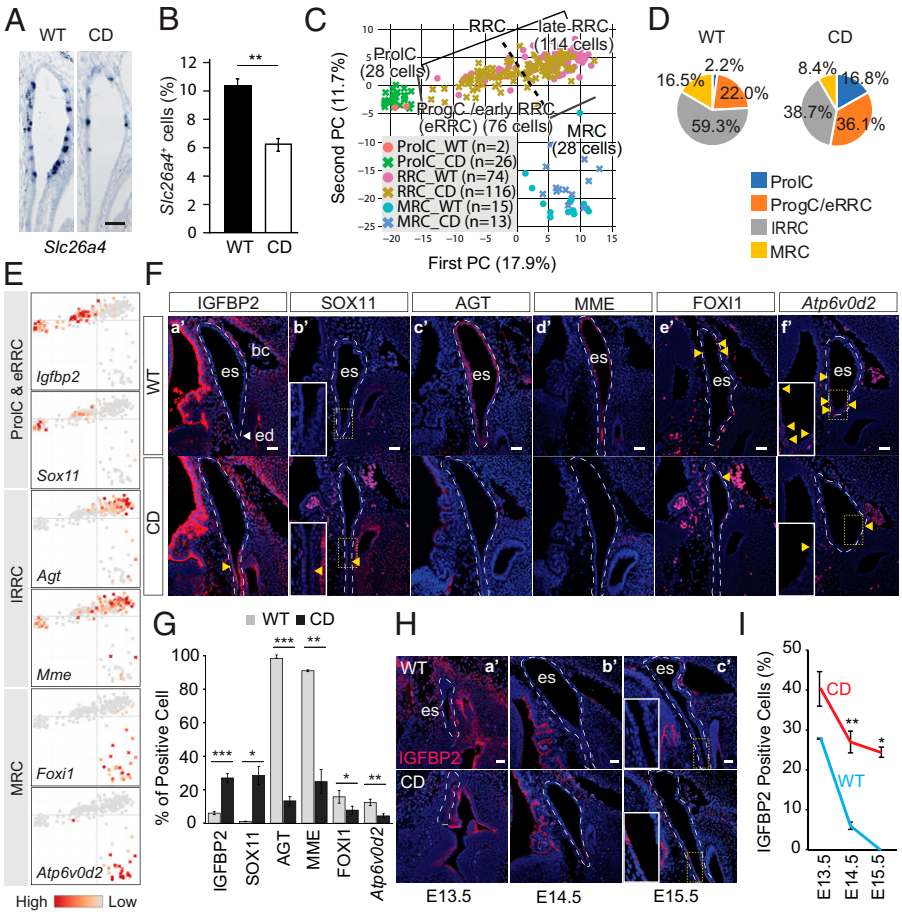

Fig. 2. Impaired differentiation in the *Sox9*$^{Y440X/+}$ (CD) ES. (*A*) *Slc26a4* expression in the ES of WT and CD mutant at E14.5 ($n = 3$). (*B*) Percentage of *Slc26a4*-expressing cells (blue in *A*) among the total number of epithelial cells ($n = 3$). (*C*) Principal component (PC) analysis of 246 cells identifies three distinctive cell populations, whereby RRCs are further divided into early (eRRCs) and late (lRRCs) ones. (*D*) Pie charts showing the proportion of cell populations per genotype. (*E*) PCA plots showing marker gene expression for each population identified. (*F*) Immunostaining or hybridization chain reaction (HCR) of population markers in the WT and CD ES at E14.5: (*F*, *a′*) IGFBP2 ($n = 3$), (*F*, *b′*) SOX11 ($n = 2$), (*F*, *c′*) AGT ($n = 2$), (*F*, *d′*) MME ($n = 2$), (*F*, *e′*) FOXI1 ($n = 3$), and (*F*, *f′*) *Atp6v0d2* ($n = 3$). (*G*) Proportion of cells (percentage) expressing markers in *F*. (*H*) Immunostaining of IGFBP2 in E13.5 to E15.5 WT and CD ES: (*H*, *a′*) E13.5 ($n = 2$), (*H*, *b′*) E14.5 ($n = 3$), and (*H*, *c′*) E15.5 ($n = 2$). (*I*) Quantification of cells (percentage) expressing IGFBP2 in E13.5 to E15.5 WT and CD ES. Data are presented as means ± SEM. Highlighted signals are indicated with yellow arrowheads. bc, blood cell; ed, ED; es, ES. (Scale bars: 50 μm in *A*; 40 μm in *F* and *H*.) *$P < 0.05$; **$P < 0.01$; ***$P < 0.001$.

transcriptomes for E12.5 and E16.5 ES (53) (*SI Appendix*, Fig. S2 *A–C*). The clusters were ProlCs (marked by *Mki67* and *Birc5*), ribosome-rich cells (RRCs; marked by *Dach2*, *Oc90*, *Agt*, and *Mme*), and mitochondrial-rich cells (MRCs; marked by *Atp6v0d2*, *Foxi1*, and *Slc26a4*). Functional annotation by gene ontology (GO) analyses was consistent with current knowledge; ProlCs were enriched in cell cycle and mitotic activities, and MRCs and RRCs were enriched in epithelial cell properties. GO for MRCs reflected the enrichment for mitochondrial activity and expression of membrane transporters and ion channels that maintain fluid homeostasis in the inner ear. For RRCs, GO reflected enrichment for cell–cell communication and the extracellular matrix (matrisome) (54) (*SI Appendix*, Fig. S2*D*). All three populations expressed genes encoding ionic transporters or membrane channels (GO: 0015075, total of 851 genes), especially RRCs and MRCs. MRCs expressed more active transporters and/or membrane channels than the other two clusters: ProlCs and RRCs (*SI Appendix*, Fig. S2*E*).

Density contour plots identified two subpopulations within the RRC cluster (*SI Appendix*, Fig. S2 *F* and *G*). One subpopulation was similar to reported immature cell types, early ribosome-rich cells (eRRCs; odds ratio = 31.4), and ProgCs (odds ratio = 44.1), which we annotated as ProgCs/eRRCs (*SI Appendix*, Fig. S2*H*). The other subpopulation was similar (odds ratio = 21.7) to reported more mature ribosome-rich cells (late RRCs, or lRRCs) (53). Genes marking the ProgCs/eRRCs include *Igfbp2*, *Aldh1a3*, and *Fam132a*, and those marking lRRCs include *Mme* and *Agt* (Dataset S1 and *SI Appendix*, Fig. S2*I*). Pseudotime trajectory plots and empirical entropy estimation predicted lineage progression from ProgCs/eRRC to RRC and then, MRC (*SI Appendix*, Fig. S2 *J–M*), consistent with the suggested lineage origin of MRC from RRCs (53).

Increased Proportion of Immature Cells in the *Sox9*$^{Y440X/+}$ ES. To examine if the *Sox9*^{Y440X} mutation affects RRCs, MRC fate, and/or differentiation progression, we compared the proportion of different cell clusters. We observed a lower proportion of MRCs (mature cells) in the mutant (8.4%) than in WT (16.5%). The proportion of lRRCs (mature cells) was also reduced by 20.6 percentage points in the mutant (Pearson χ^2 $P = 0.003$) compared with WT. By contrast, the proportion of immature cells increased (ProlCs [14.6 percentage points] and ProgCs/eRRCs [14.1 percentage points]) in the mutant (Pearson χ^2 $P = 0.001$ and $P = 0.029$, respectively) (Fig. 2 *C* and *D*), resulting in a deficiency in mature cells.

To assess whether this deficiency was associated with differentiation states, we assessed the sequence of differentiation in the ES. IGFBP2 and SOX11 mark ProlCs/eRRCs at the proximal end of the ES. AGT and MME mark lRRCs, while FOXI1 and *Atp6v0d2* mark MRCs. Both cell types are evenly distributed with more lRRCs in the sac (Fig. 2 *E* and *F*). Quantification of these different cell types confirmed the reduced proportions of mature cells (lRRCs and MRCs) vs. immature cells in the mutant compared with WT (Fig. 2*G* and *SI Appendix*, Table S1). FOXI1 directly transactivates *Slc26a4* (49). In line with the reduced proportion of *Slc26a4*$^+$ cells (Fig. 2 *A* and *B*), there were fewer *Foxi1*-expressing cells (8% in mutants vs. 16% in WT) (*SI Appendix*, Table S1). However, transcript levels for both genes were comparable in the MRCs of both genotypes (Fig. 2*A* and *SI Appendix*, Fig. S2*N*), suggesting that the reduced proportion of *Slc26a4*$^+$ cells was not due to the down-regulation of FOXI1.

Analyses of our data and published single cell RNA sequencing (scRNA-seq) data (53) suggest that lRRCs and MRCs originate from ProgCs/eRRCs (*SI Appendix*, Fig. S2 *J* and *K*), which are *Igfbp2*$^{+}$. We assessed the number of IGFBP2^{+} cells from E13.5 to E15.5 in the WT and mutant ED. While the proportion of WT IGFBP2^{+} between E13.5 and E15.5 reduced from 27.8 to 0%, in mutants the frequency of these cells was significantly higher at all stages (E13.5 [40. 3%]) and at E14.5 and E15.5, remained at 27.0 and 24.4%, respectively (Fig. 2 *H* and *I*), suggesting that differentiation was delayed. *Sox11* is essential for inner ear development (55) and is expressed by E12.5 ES progenitors (53). Consistent with our hypothesis of delayed differentiation, we found that *Sox11* expression in the mutant ProlCs/ProgCs/eRRCs persisted in the mutant ES/ED at E14.5 (Fig. 2 *E* and *F*).

Dysregulated Genes Regulating Fluid Regulation, Cell–Cell Interaction, and Wnt Signaling in *Sox9*$^{Y440X/+}$ RRCs. We next identified DEGs in RRCs caused by *Sox9*^{Y440X}. Over a hundred DEGs (103 genes) were found between WT and mutants (Fig. 3*A*, Dataset S1, and *SI Appendix*, Fig. S3*A*), of which 58 genes were also DEGs in RRCs against all cell clusters (odds ratio = 94.6, Pearson χ^2 $P < 2.2 \times 10^{-16}$). Functional annotation (GO) of genes down-regulated in mutant RRCs identified processes related to extracellular structure organization, sensory organ and ear/otolith development, and neurogenesis, while the up-regulated genes were associated with cell junctions and cell–cell adhesion (*SI Appendix*, Fig. S3*B*). Importantly, several genes involved in fluid regulation were down-regulated in the *Sox9*$^{Y440X/+}$ mutant ES, such as genes encoding ion transporters (e.g., *Slc24a4* and *Slc15a1*), channels (*Ttyh1*), gap junction protein (*Gjb2*), and members of the renin-angiotensin system (e.g., *Mme*, *Agt*) (Fig. 3*A*, Dataset S1, and *SI Appendix*, Fig. S3 *A*, *C*, and *D*). These changes are consistent with the observed ear hydrops. Genes associated with the Wingless-related integration site (Wnt) pathway were also affected. *Dkk3*, a Wnt antagonist, was down-regulated, while Wnt targets and ligands *Ccnd2* and *Wnt6*/*10a* were up-regulated in the mutant (Fig. 3*A*, Dataset S1, and *SI Appendix*, Fig. S3*A*). Coexpression analyses confirmed that *Ccnd2*, *Wnt6*, and *Igfbp2* were negatively correlated with *Dkk3*, indicating a coordinated dysregulation and a net up-regulation of the pathway (*SI Appendix*, Fig. S3*E*).

***Sox9*^{Y440X} Impacts *Sox10* Expression and Its Regulon.** *Sox10* expression is initiated later than *Sox9* expression in the mouse otic placode and is absent in conditional *Sox9*-null otocysts (18). *Sox10* is coexpressed with *Sox9* in the otic epithelium (19, 56). Strikingly, expression of *Sox10* was highly affected by the *Sox9*^{Y440X} mutation in the RRCs (Fig. 3 *A* and *B*). Almost all ES/ED cells express SOX10 from E13.5 to E15.5. However, the proportion of SOX10^{+} cells in the mutant was low and decreased from 27.2% at E13.5 to less than 20% at E15.5 (*SI Appendix*, Fig. S3*F*). Single-Cell Regulatory Network Inference and Clustering (SCENIC) regulon analysis also identified reduced SOX10 activity in the mutant RRCs (*SI Appendix*, Fig. S3*G*). Transcriptional targets (*Oc90*, *Dkk3*, and *Nox3*) of the SOX10 regulon, known to be critical for ES/inner ear function, were affected (Fig. 3 *C*–*E*).

SOX factors interact with a range of partners, allowing for individual factors to regulate different genes and alternative developmental programs (2, 37, 57, 58). β-catenin activates gene expression via interaction with T-cell factor/lymphoid

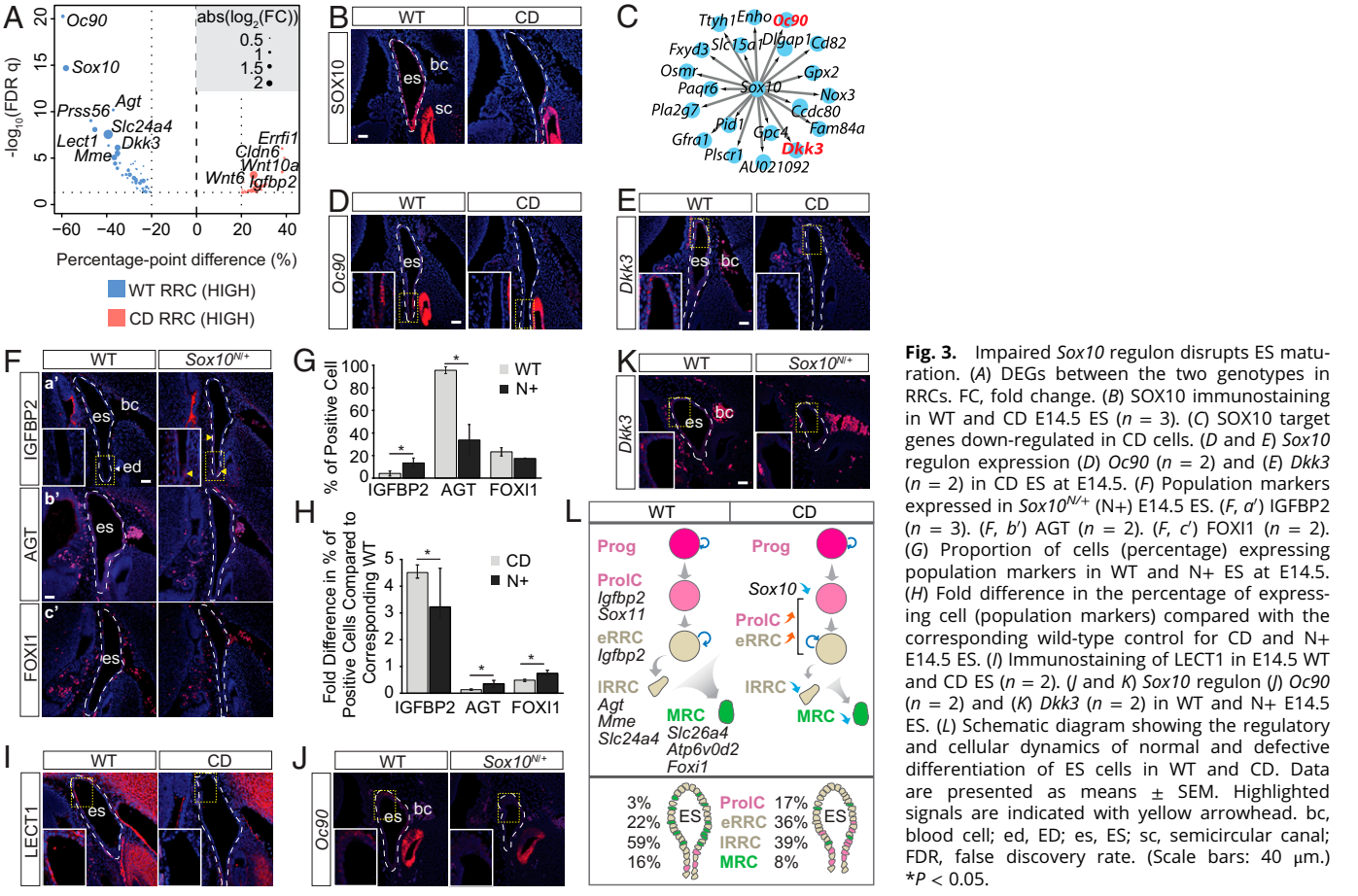

Fig. 3. Impaired *Sox10* regulon disrupts ES maturation. (*A*) DEGs between the two genotypes in RRCs. FC, fold change. (*B*) SOX10 immunostaining in WT and CD E14.5 ES ($n = 3$). (*C*) SOX10 target genes down-regulated in CD cells. (*D* and *E*) *Sox10* regulon expression (*D*) *Oc90* ($n = 2$) and (*E*) *Dkk3* ($n = 2$) in CD ES at E14.5. (*F*) Population markers expressed in *Sox10*$^{N/+}$ (N+) E14.5 ES. (*F*, *a'*) IGFBP2 ($n = 3$). (*F*, *b'*) AGT ($n = 2$). (*F*, *c'*) FOXI1 ($n = 2$). (*G*) Proportion of cells (percentage) expressing population markers in WT and N+ ES at E14.5. (*H*) Fold difference in the percentage of expressing cell (population markers) compared with the corresponding wild-type control for CD and N+ E14.5 ES. (*I*) Immunostaining of LECT1 in E14.5 WT and CD ES ($n = 2$). (*J* and *K*) *Sox10* regulon (*J*) *Oc90* ($n = 2$) and (*K*) *Dkk3* ($n = 2$) in WT and N+ E14.5 ES. (*L*) Schematic diagram showing the regulatory and cellular dynamics of normal and defective differentiation of ES cells in WT and CD. Data are presented as means ± SEM. Highlighted signals are indicated with yellow arrowhead. bc, blood cell; ed, ED; es, ES; sc, semicircular canal; FDR, false discovery rate. (Scale bars: 40 μm.) *$P < 0.05$.

enhancer factor (TCF/LEF) transcription factors. SOX9, through its C-terminal transactivation domain, interacts physically with β-catenin, stimulates its degradation, and inhibits TCF/LEF gene activation (59, 60). The truncation of SOX9 at Y440 deletes most of the interacting domain (amino acids 382 to 509) and likely compromises the inhibitory activity of SOX9 on β-catenin. The increase in LEF regulon activity observed in lRRCs and MRCs supports the notion that SOX9 and TCF/LEF compete for binding to β-catenin (59). Differential gene expression analyses and marker analyses indicate dysregulation of Wnt signaling in the $Sox9^{Y440X/+}$ mutant ES as reflected by changes in pathway-associated genes, such as *Gjb2*, *Wnt6*, *Wnt10a*, *Ccnd2*, and *Dkk3*. Interestingly, there are two conserved enhancers in the *Sox10* locus that are active in the chick otic vesicle, one of which bears SOXE binding sites with overlapping TCF/LEF sites (24, 25), consistent with the possibility of impaired WNT signaling control of *Sox10*. In skeletogenic cells, SOXC proteins, such as SOX11, contribute to the synergistic stabilization of β-catenin and negative regulation of *Sox9* (61), which raises the question about the contribution of *Sox11* to persisting progenitors in the $Sox9^{Y440X/+}$ ES/ED and to the dysregulation of canonical Wnt signaling.

SOXE genes act dosage dependently (62). We asked to what degree the downstream gene expression changes were attributable to down-regulation of *Sox10* and/or impaired SOX9 function. As in $Sox9^{Y440X/+}$ mutants but to a lesser degree, more $IGFBP2^{+}$ cells (~10%) were present in the E14.5 ES/ED of $Sox10^{N/+}$ (*Sox10*-null) mutants than in WT, suggesting that reduced SOX10 levels contribute to the persistence of IGFBP2+ progenitors in $Sox9^{Y440X/+}$ mutants. There was also a corresponding decrease in the proportion of mature RRCs and MRCs identified by their expression of *Agt* and *Foxi1*, respectively (Fig. 3 *F–H* and *SI Appendix*, Table S2). *Chondromodulin* (*Lect1*), a known downstream target of SOX9 in chondrocytes (63, 64), was strongly down-regulated in the $Sox9^{Y440X/+}$ mutant RRCs/ES (Fig. 3 *A* and *I*) but unaffected in $Sox10^{N/+}$ mutant ES/ED cells (*SI Appendix*, Fig. S3*H*). We hypothesize that $SOX9^{Y440X}$ impacts the ES/ED cells by specific effects on SOX9 direct targets (e.g., on *Lect1* and *Sox10*) combined with downstream changes caused by down-regulation of SOX10. For example, *Oc90* and *Dkk3* are down-regulated not only in $Sox9^{Y440X/+}$ but also, in $Sox10^{N/+}$ mutants (Fig. 3 *J* and *K*) and may be common targets. By contrast, expression of the SOX9 target *Lect1* was unaffected in $Sox10^{N/+}$ ES/ED, suggesting that it is not regulated by SOX10. The more severe impact of the $SOX9^{Y440X}$ mutation could be caused by the combined failure of SOX9 to activate its own specific target genes and impaired maintenance of *Sox10* expression. Together, these changes culminate to disrupt the differentiation of mature cells (RRCs and MRCs) for proper ES/ED function (Fig. 3*L*).

***Sox9* and *Sox10* Interact Genetically, with $Sox9^{Y440X}$ Exerting the Most Severe Effects.** SOX proteins work dose dependently (37). To gain insight into the functional relationship between *Sox9*, *Sox10*, and gene dosage effects, we studied the genetic interaction between *Sox9* and *Sox10* in single and compound mutants: conditional heterozygous *Sox9*-null mutant ($B2\text{-}Sox9^{c/+}$), conditional heterozygous $Sox9^{Y440X}$ mutant ($B2\text{-}Sox9^{cY440X/+}$), hetero- and homozygous *Sox10*-null mutants $Sox10^{N/+}$ and $Sox10^{N/N}$, compound heterozygous conditional *Sox9*-null and *Sox10*-null mutants ($B2\text{-}Sox9^{c/+};Sox10^{N/+}$), and compound heterozygous $Sox9^{Y440X}$ and *Sox10*-null mutants ($B2\text{-}Sox9^{cY440X/+};$

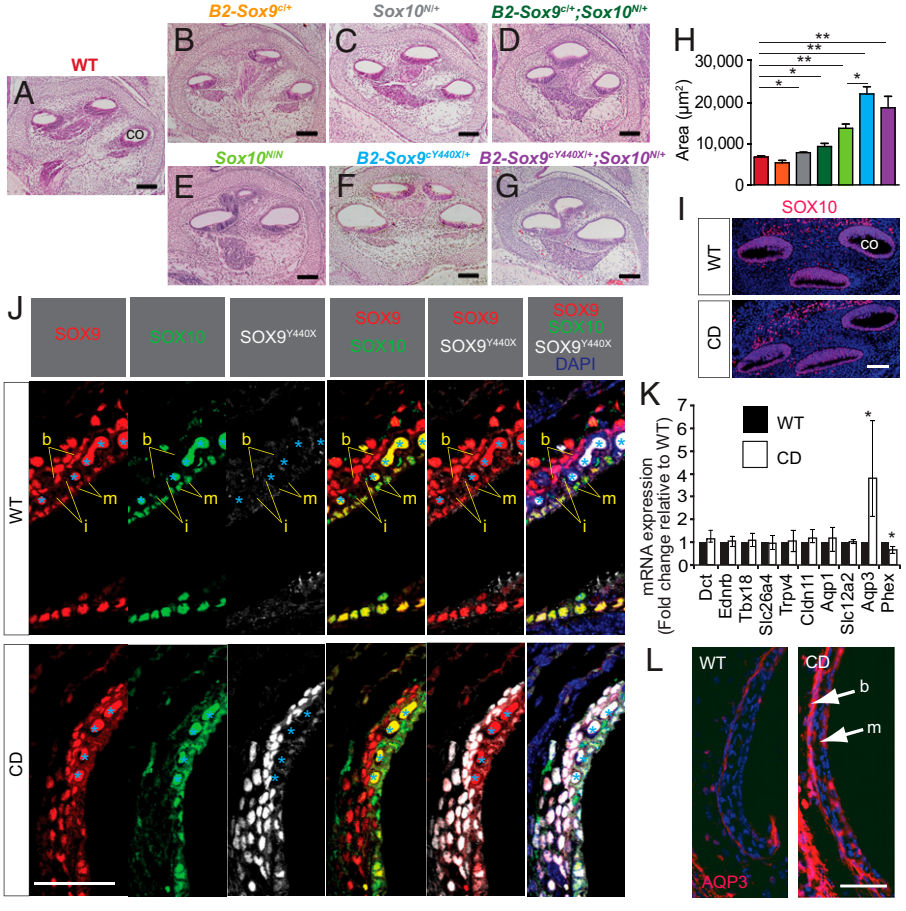

Fig. 4. Prenatal hydrops in SoxE mutant cochleae and increased *Aqp3* expression in the $Sox9^{Y440X/+}$ (CD) mutant. (*A–G*) Histology of WT and SoxE mutant cochleae at E15.5 (n = 4 to 5). (*H*) Basal cochlear luminal area measured for cochleae in *A–G* (n = 4 to 5). (*I*) Immunostaining of SOX10 in WT and CD cochlea at E14.5 (n = 3). (*J*) Immunostaining of SOX9, SOX10, and $SOX9^{Y440X}$ in WT and CD stria vascularis at P5 (n = 2). Blood cells are indicated by light blue asterisks. DAPI, 4′,6-diamidino-2-phenylindole. (*K*) Relative messenger RNA (mRNA) expression (normalized to *Hprt*) of candidate SOX9 targets in P3 cochleae by qRT-PCR (n = 3). (*L*) Increased expression of AQP3 in the marginal and basal layers of stria vascularis of CD mutant cochlea at P3 shown by immunostaining (n = 2). Data are presented as means ± SEM. b, basal cell; co, cochlea; i, intermediate cell; m, marginal cell. (Scale bars: 100 μm in *A–G*; 40 μm in *I*, *J*, and *L*.) *P < 0.05; **P < 0.01.

Sox10$^{N/+}$). Using the area of the basal cochlea lumen as the readout revealed significant enlargement in some of the mutants (Fig. 4 *A*–*G*). At E15.5, the area of the basal cochlea lumen was normal in the *B2-Sox9*$^{c/+}$ mutant (Fig. 4*B*), suggesting that haploinsufficiency for SOX9 was not responsible for the enlargement. However, the lumen was larger in both *Sox10*$^{N/+}$ ($P < 0.05$) (Fig. 4*C*) and *B2-Sox9*$^{c/+}$;*Sox10*$^{N/+}$ mutants ($P < 0.05$) (Fig. 4 *D* and *H*), but there was no statistical difference in the basal lumen area between *Sox10*$^{N/+}$ and *B2-Sox9*$^{c/+}$;*Sox10*$^{N/+}$ mutants suggesting haploinsufficiency for SOX10 as the cause of enlargement. However, the basal lumen area was increased 3.2 times ($P < 0.01$) for *B2-Sox9*$^{cY440X/+}$, 2.0 times ($P < 0.01$) for *Sox10*$^{N/N}$, and 2.7 times ($P < 0.01$) for *B2-Sox9*$^{Y440X/+}$;*Sox10*$^{N/+}$ compared with WT (Fig. 4 *E*–*G*). The *Sox10*$^{N/+}$ allele in combination with *Sox9*$^{cY440X/+}$ did not significantly exacerbate the lumen enlargement ($P = 0.4$), whereas the impact of *Sox9*$^{cY440X/+}$ was significantly greater than for *Sox10*$^{N/N}$ ($P = 0.01$). Overall, *Sox9*^{Y440X} alone resulted in the most severe hydrops, raising the possibility that it may interfere in a dominant manner with normal SOX9 and SOX10 function. Consistent with this notion is the lack of auditory and vestibular deficits in the otic conditional *Sox9*-null mutant (*B2-Sox9*$^{c/+}$) (*SI Appendix*, Fig. S4 *H*–*K*) in contrast to B2-Sox9$^{cY440X/+}$ mutants.

AQP3 Is Derepressed in the Postnatal *Sox9*$^{Y440X/+}$ Stria Vascularis. We asked whether *Sox10* was also down-regulated in the E14.5 cochlea. Unexpectedly, despite the presence of SOX9^{Y440X} protein in the cochlea (Fig. 1*C*), SOX10, LECT1, and MME expressions were unaffected at E14.5 (Fig. 4*I* and *SI Appendix*, Fig. S5 *A* and *B*), even though the genes encoding these proteins were down-regulated in the ES. Since the ES/ED is continuous with the cochlea, the enlarged cochlea lumen may be a secondary consequence of dysregulated ionic/fluid balance in the ES/ED starting from E15. The reason for the divergent impact of SOX9^{Y440X} on *Sox10* in the ES and E14.5 cochlea is unclear. Expression of the mutant allele and SOX9^{Y440X} protein in the ES/ED appeared higher than in the cochlea. The contrasting effect on the cochlea could be due to the lower SOX9^{Y440X} protein expression in the E14.5 cochlea epithelium compared with the cartilaginous capsule, where high levels of SOX9^{Y440X} were detected (Fig. 1C) and LECT1 expression was down-regulated (*SI Appendix*, Fig. S5*A*).

The stria vascularis is essential for generating endocochlear potential, develops later in inner ear development, and matures at postnatal stages around P3. There are three distinct cell layers of the stria vascularis: the marginal layer derived from the otic epithelium, the intermediate layer composed of melanocytes, and the basal layer derived from the otic mesenchyme. Basal cells express both SOX9 and SOX9^{Y440X} proteins. SOX9/SOX9^{Y440X} are coexpressed with SOX10 in the marginal cells, while the intermediate cells express only SOX10 (Fig. 4*J* and *SI Appendix*, Fig. S5*F*). Given the marked swelling of the scala media in adults (Fig. 1 *I* and *J*) and the expression of SOX9 and SOX10, it was possible that these factors have a later function in addition to the ES/ED, and molecular changes could occur as the stria vascularis matures that could impact endocochlear function. All three layers developed in *Sox9*$^{Y440X/+}$ mutants as identified by corresponding marker proteins (*SI Appendix*, Fig. S5 *C*–*E*). We examined genes for the following: ion channels; cotransporters, and water channels (*Slc12a2*, *Trpv4*, *Aqp1*, *Aqp3*); genes expressed by melanocytes (*Ednrb*, *Dct*); factors important for fibrocyte development (*Tbx18*); tight junction components (*Cldn11*); and genes in which mutations cause hydropic ears (*Slc26a4*, *Phex*) by qRT-PCR. Among these, *Phex*, a reported SOX9 target (65), was down-regulated, while *Aqp3* was found to be significantly up-regulated, with a four-time increase in the *Sox9*$^{Y440X/+}$ mutant cochlea as compared with the WT (Fig. 4*K*). AQPs transport water molecules across the plasma membrane and are essential for the establishment and maintenance of the inner ear fluid. Their dysregulation has been implicated in the development of endolymphatic hydrops in mice (66) and humans, and they are potential drug targets for the condition (67, 68). Immunostaining confirmed stronger signals for AQP3 in both marginal and basal cell layers in the mutant compared with WT (Fig. 4*L*), which could contribute to unbalanced fluid transport to the ductal lumen and fluid accumulation. These data also raise the possibility that SOX9^{Y440X} may dominantly interfere with SOX9 and SOX10 cooperation in the marginal and basal layers.

SOX9 and SOX10 Bind Cooperatively to an *Aqp3* Cis-Regulatory Element. The genetic interaction between *Sox9* and *Sox10* mutants (Fig. 4) raised the possibility that the two factors cooperate molecularly in regulating transcription, which leads us to hypothesize that this cooperation would be relevant for those targets, such as *Aqp3*, that harbor regulatory elements that can bind both SOXE factors. We asked whether SOX9 and SOX10 could both regulate *Aqp3* directly. We identified a functional in vivo SOX9 binding site [COL2C2 (69)] in a conserved region in intron 1 of *Aqp3* (70) (*SI Appendix*, Fig. S6 *A* and *B*). Three SOX10 binding sites were predicted in the region using motifs of the JASPAR database (71, 72) (Fig. 5*A* and *SI Appendix*, Fig. S6 *A* and *B*) and overlap with a The Encyclopedia of DNA Elements (ENCODE) candidate cis-regulatory element. By chromatin immunoprecipitation (ChIP) qPCR assays, we found that SOX9 and SOX10 bound DNA fragments containing the SOX9/SOX10 binding sites in the *Aqp3* locus (Fig. 5*B*) but not unrelated sequences (negative control, *Crygb*), suggesting that SOX9 and SOX10 directly regulate *Aqp3*.

To test whether SOX9 and SOX10 are physically associated, we tested for positive cooperativity for interactions by electrophoretic mobility shift assays (EMSAs) with protein constructs purified to homogeneity (36) (Fig. 5*C*). We selected a sequence with a palindromic (reverse–forward) configuration of canonical *SOX* half-sites (termed the "CD-Rap" motif) (73) (Fig. 5*D*). We also tested probes encoding the *Aqp3* SOX9–SOX10 motif harboring a COL2C2-like SOX9 site juxtaposed to a degenerate SOX10 binding site, which resembles a hitherto unknown "forward–forward" configuration with an 11–base pair spacer. High mobility group (HMG) box constructs devoid of the dimerization domain migrated predominantly as monomers on both the canonical CD-Rap and the *Aqp3* element (*SI Appendix*, Fig. S6 *C* and *D*). By contrast, the SOX9-NHMG (N terminus to HMG) and SOX10-DIM (dimerization) constructs, including the dimerization domains, migrated predominantly as dimers, indicating highly cooperative homodimerization that depends on the presence of the DIM domain (Fig. 5 *E*–*G*).

We next asked whether SOX9 and SOX10 could form heterodimers on the noncanonical *Aqp3* element. We incubated canonical or *Aqp3* EMSA probes simultaneously with SOX9 and SOX10 protein constructs, both of which contain the DIM domain but that are of different lengths, such that the various protein/DNA complexes are discernible on EMSA gels (Fig. 5 *C* and *H*). On both motifs, we observed prominent SOX9/SOX10 complexes as well as homodimeric SOX9/SOX9 or SOX10/SOX10 complexes (Fig. 5*H*). These biophysical/biochemical interaction assays suggest that SOX9 and SOX10 can form highly cooperative homodimers as well as heterodimers

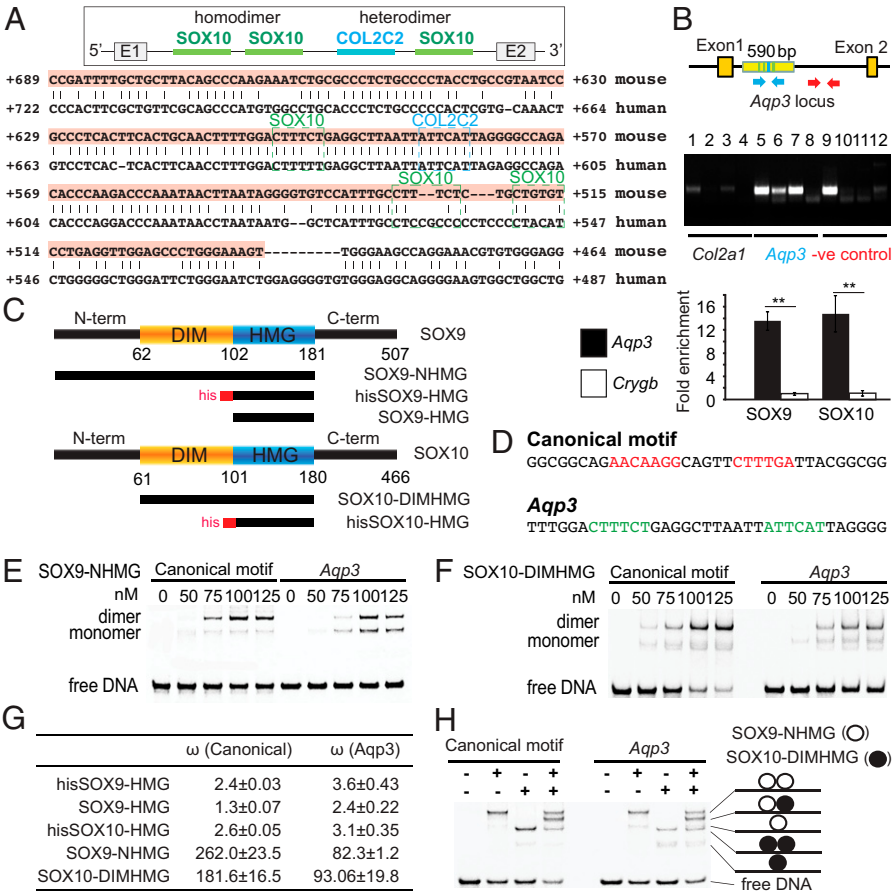

Fig. 5. *Aqp3* is potentially regulated by SOXE dimers with strong positive cooperativity. (*A*) Conserved SOX9 and SOX10 binding sites predicted by bsConserve and Jasper over a 205-bp conserved noncoding region by Vista in intron 1 of *Aqp3*. A COL2C2 (ATTCAT) SOX9 binding site (69) is detected in intron 1. COL2C2 and SOX10 binding sites are boxed in blue and green, respectively. (*B*) ChIP assays for SOX9 and SOX10 on the WT inner ear at E14.5 ($n = 2$). *Col2a1* (positive control) is the known SOX9 binding region. Arrows in blue indicate primer sites flanking the *Aqp3* intron 1 region with predicted SOX9 and SOX10 binding sites. Arrows in red indicate primer sites flanking 1 kb downstream of the predicted SOX9 or SOX10 binding site. Real-time PCR-amplified DNA fragments were immunoprecipitated by SOX9 or SOX10 antibody, the *Aqp3* intron1 region (blue arrows), or the *Crygb* (gamma-b-crystallin) promoter (negative control; $n = 3$). Lanes 1, 5, and 9: genomic DNA (gDNA); lanes 2, 6, and 10: α-SOX10 antibody (Ab); lanes 3, 7, and 11: α-SOX9 Ab; lanes 4, 8, and 12: control serum. (*C*) Domain composition of SOX9 and SOX10 proteins and (*D*) DNA sequences of oligos used in EMSAs. (*E*) The SOX9-NHMG and (*F*) SOX10-DIMHMG constructs containing the DIM domain dimerized with strong positive cooperativity ($n = 4$). (*G*) The homodimer cooperativity factors were estimated as described (98, 99). (*H*) SOX9 and SOX10 proteins heterodimerized effectively on the *Aqp3* sequences ($n = 4$). -, not added. +, added. Data are presented as means ± SEM. $^{**}P < 0.01$.

on the *Aqp3* enhancer DNA. This suggests that both proteins work together to suppress *Aqp3* expression. Whether possible bindings of SOX9 homodimers, SOX10 homodimers, and SOX9–SOX10 heterodimers are interchangeable is an important question to address in the future.

SOX9^{Y440X} Compromises Cooperative Repression of *Aqp3* by SOX9 and SOX10. The inappropriate expression of AQP3 in the stria vascularis led us to hypothesize that SOX9 and SOX10 can repress *Aqp3* expression in part via the first intron element. We, therefore, investigated the effect of SOX9, SOX9^{Y440X}, and SOX10 on regulation of the *Aqp3* gene. We constructed a 590-base pair (bp) reporter vector from intron 1 of *Aqp3* (Aqp3-Luc-23) containing a 205-bp sequence harboring the heterodimer site with an 11-bp spacing and one SOX10 homodimer site with 3-bp spacing. Aqp3-Luc-23 was transfected into mouse inner medullary collecting duct (mIMCD) cells, which express high levels of *Aqp3* but little *Sox9* and *Sox10* and are, therefore, suitable for testing the inhibitory effect of SOXE factors. Higher luciferase expression was observed in cells transfected with the reporter construct compared with cells transfected with the empty luciferase plasmid (Fig. 6*A*). Hence, the fragment acted like an enhancer for *Aqp3* in cells expressing the gene. However, when Aqp3-Luc-23 was transfected together with an SOX9 or SOX10 expression construct, luciferase reporter activity was inhibited, with SOX9 exerting a stronger negative effect. Transfection of SOX9^{Y440X} with Aqp3-Luc-23 had no effect (Fig. 6*B*). Cotransfection of expression constructs for SOX9^{Y440X} and SOX9 reversed the inhibition of *Aqp3* expression and even increased it above control levels when the SOX9^{Y440X} concentration was twice the amount of SOX9 (Fig. 6*C*). This result suggests that the competition of SOX9 and SOX9^{Y440X} proteins in binding to the *Aqp3* regulatory element allows some transactivation activity. The transactivation effect of SOX9^{Y440X} on reporter expression was inhibited by SOX10 dose dependently (Fig. 6*D*). Collectively, our results suggest that SOX9^{Y440X} and WT SOX9/10 factors compete with one another to regulate *Aqp3*.

Neither SOX9 nor SOX10 were able to suppress the reporter activity in mIMCD cells when the SOX9 in vivo binding consensus (COL2C2-like sequence site) (69) or the SOX10 binding sites were mutated (Fig. 6 *E* and *F* and *SI Appendix*, Fig. S6 *E* and *F*). Interestingly, when the COL2C2 site was mutated, expression of SOX9^{Y440X} resulted in transactivation of the reporter. Similarly, transactivation of the reporter was increased when the SOX10 site was mutated, consistent with the requirement for both SOXEs for inhibition. These results may reflect

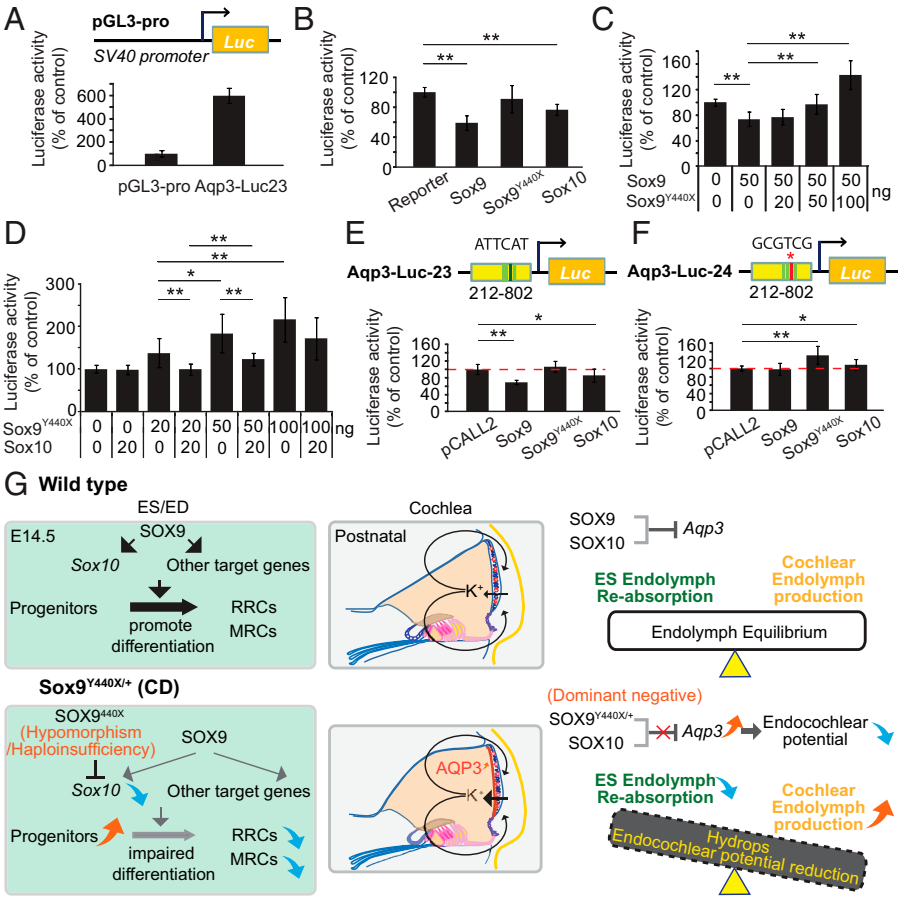

Fig. 6. SOXE regulation of *Aqp3* expression and development of the endolymphatic system. (*A–F*) Impact of SOXE and SOX9^{Y440X} on *Aqp3* regulatory element–driven luciferase reporter transactivation. (*A*) Reporter activity of the expression vector comprising the fragment of intron 1 of *Aqp3* (+212 to +802) with SOX9 and SOX10 binding sites, driving expression of a luciferase reporter pGL3-pro (Aqp3-Luc-23), in mIMCD3 cells (n = 3). (*B*) Impact of SOX9, SOX9^{Y440X}, and SOX10 on Aqp3-Luc-23 activity. Luciferase activity was normalized to activity with the reporter only. SOX9 but not SOX9^{Y440X} dampened reporter activity by 40% (n = 3). (*C*) The effect of increasing amounts of *Sox9*^{Y440X} expression vector (0 to 100 ng) on *Sox9* expression vector (50-ng) inhibition of Aqp3-Luc23 activity. SOX9 inhibition of reporter was reversed by increasing concentrations of transfected *Sox9*^{Y440X} (n = 3). (*D*) Effect of increasing amounts of *Sox9*^{Y440X} expression vector (0 to 100 ng) on *Sox10* expression vector (20-ng) inhibition of Aqp3-luc23. SOX9^{Y440X} overcame SOX10 inhibition of Aqp3-luc23 (n = 3). (*E* and *F*) SOX9 and SOX10 inhibition of Aqp3-luc23 activity was abolished when the SOX9 binding site COL2C2 was mutated (from ATTCAT to GCGTCG [red asterisk]; Aqp3-luc24; n = 3). (*G*) Model of SOXE control of endolymphatic development and the impact of SOX9^{Y440X} mutation on inner ear fluid homeostasis via two independent mechanisms in the cochlea and ES. Data are presented as means ± SEM. *P < 0.05; **P < 0.01.

partial recovery of the enhancer activity due to the reduced binding of SOX9 and altered interactions with partner factors via the truncated transactivation domain. Overall, the data suggest that the specific binding sequences are critical for the inhibition of *Aqp3* expression by SOX9 and SOX10, which is mediated in part by the activity of heterodimers in concert with appropriate partner factors (Fig. 6*G*).

Discussion

Defining in vivo cellular and molecular mechanisms underlying dominant syndromic disorders is complicated by unclear genotype–phenotype correlations and compensatory or dominant negative effects in multiple affected tissues. This is particularly relevant where heterozygosity involves a mutation that could lead to both hypomorphic and dominant effects in a developmentally important transcription factor, such as SOX9. While SOX9 and SOX10 are coexpressed in the inner ear and other cell types, such as the neural crest, SOX9, but not SOX10, is expressed in chondrocytes. Heterozygosity for SOX9 causes endochondral bone defects (29), which are not seen in the *Sox10*^{Dom} mutants (74, 75), consistent with independent roles for each SOXE factor. In mouse, *Xenopus*, and zebrafish, complete loss of either *Sox9* or *Sox10* impacts otic development (18, 20, 76). SOX9 and SOX10 have both transactivator and repressor activity depending on the target gene and cell type (1, 77, 78), although such activity has not been demonstrated in the inner ear. Another level of complexity is that SOXE works in various dimer configurations and partners with other factors to regulate gene expression (37, 38). To gain insights into mechanisms, we have addressed the impact of heterozygosity for SOXE mutations, singly and in combination, when either or both of them are mutated by studying three types of mutations: heterozygous null mutations in both *Sox9* and *Sox10* and the Y440X truncating mutation in *Sox9*, which gives a CD phenotype different from that of the null.

A key finding is the lack of inner ear phenotype in heterozygous conditional *Sox9*$^{+/-}$-null mutants. This suggests that haploinsufficiency for SOX9 is not the underlying cause of the inner ear defects and implicates instead a dominant negative or neomorphic mode of action for SOX9^{Y440X}. The impact of *Sox9*^{Y440X} on enlargement of the cochlear lumen was more marked than for *Sox10*$^{N/+}$ (which must be haploinsufficient), consistent with a dominant negative impact of SOX9^{Y440X} on *Sox10* itself, on SOX10 target genes, and also, on other targets regulated by SOX9 independent of SOX10. The differing impact of the *SOX9*^{Y440X} mutation in two critical structures of the inner ear, the ES and the stria vascularis, could also implicate

hypomorphic effects in the former and dominant negative effects in the latter, which combine to affect the development of the endolymphatic system and the later maintenance of fluid homeostasis/endocochlear potential and thereby, hearing.

We have provided in vivo genetic evidence for the essential roles of cooperation of SOX9 and SOX10 in controlling the development of the endolymphatic system and the ionic composition of the endolymph. We found that these SOXE factors function early in the developing ES/ED. SOX9 has a critical role in maintaining *Sox10* expression and the timely differentiation of progenitors as well as controlling the expression of genes important for ionic homeostasis. The major impact of heterozygosity or homozygosity for *Sox10* deficiency in the mouse inner ear is on the survival of progenitors in the cochlea, but no gross defects were observed in the ES of these mutants (20). Notably, different hypomorphic mutations in *Sox10* that impair the transactivation domain or DNA-dependent dimerization impact distinctive aspects of satellite glia and Schwann cells development (79). Our study shows that, compared with $Sox9^{Y440X}$, a similar, albeit more mild differentiation delay was seen in the heterozygous *Sox10*-null ES/ED, suggesting that hypomorphism/haploinsufficiency for SOX10 contributes to the developmental defect but is not solely responsible for those seen in the $Sox9^{Y440X/+}$ inner ear. The different impact of $SOX9^{Y440X}$ vs. deficiency for SOX10 (in $Sox10^{N/+}$ mutants) on the expression of *Lect1* (a known direct target of SOX9 in chondrocytes) in the ES/ED (64) highlights independent targets for each SOXE factor. The lack of impact of $SOX9^{Y440X}$ on *Lect1* expression in the cochlea correlated with lower levels of protein expression as compared with the ES/ED and chondrocytes, suggesting that the impact may depend on the level of expression of the mutant protein. The reduction of *Sox10* expression may also be exacerbated by decreased levels of SOX10 protein since its transcription is autoregulated, at least in some cell types (80).

The differential impact on *Sox10* expression level in the $Sox9^{Y440X}$ ES/ED vs. the cochlea may be related to developmental stage/cell-type differences in *Sox10* enhancer utilization (25). The level and cell type–restricted expression of *Sox9* are regulated by many enhancers distributed over 2 Mb of the genome (81). These enhancers control the exquisite sensitivity of the phenotype to levels of *Sox9* expression. The divergent levels of expression of $Sox9^{Y440X}$ seen in the ES/ED, cochlear, and cartilage may be controlled by separable enhancers. The different phenotypic impact may be attributable to differing sensitivity to perturbation in SOX9 dosage and activity similar to the neural crest (81).

Our molecular data and analyses on the postnatal stria vascularis indicate that SOX9 and SOX10 cooperate and may function as heterodimers as well as homodimers in vivo. Therefore, multiple modes of regulation by SOX9 and SOX10 may operate to maintain appropriate gene expression in the inner ear. Both transactivation and repression activity for SOXE factors have been reported in cells and in vivo models (77, 78, 82–86), although such activity has not been demonstrated in the inner ear. Here, we provide evidence that for a target gene that harbors binding regions for both SOX factors, SOX9 and SOX10 cooperate to repress *Aqp3* expression in postnatal stria vascularis; this is another example of context-dependent transactivation and repression activity of SOXE (1, 77, 78). Canonical SOXE dimers predominantly activate genes (57). Yet, in the context of the noncanonical *Aqp3* element, we observe transcriptional repression. Such regulation in vivo may involve possible interchangeable binding of SOX9 homodimers, SOX10 homodimers, and SOX9–SOX10 heterodimers in repressing *Aqp3* expression. Dimerization of SOXE is mediated by reciprocal interactions between DIM and HMG box domains (36). Because the truncated C terminus is far away from the dimerization domain, it is unlikely that Y440X changes whether $SOX9^{Y440X}$ directly interferes with SOX9:SOX10 heterodimerization or SOX9 homodimerization in vivo. Rather, $SOX9^{Y440X}$ likely impacts interactions with appropriate partner factors.

Where *Sox9* is expressed in the stria vascularis basal layer but not *Sox10* (87), SOX9 may act alone in these cells to inhibit *Aqp3* expression, but this inhibition is impaired in $Sox9^{Y440X/+}$ either by interference with cofactor/partner interaction or by haploinsufficiency/hypomorphism. In WT, *Sox9* and *Sox10* are both expressed in the marginal cells (87), and *Aqp3* expression is completely absent; however, its expression is derepressed when $SOX9^{Y440X}$ is present. Here, $SOX9^{Y440X}$ may also interfere with the cooperation of SOX9 and SOX10 in directly repressing transcription of *Aqp3*. Whether such cooperation operates in vivo via combinations of heterodimers and homodimers, and the degree with which these are additive and/or redundant is unclear. Whether a target gene is regulated by SOXE dimers and monomers in vivo is also probably dependent on the appropriate binding regions for these factors in the target gene. Questions for the future are to what extent the $SOX9^{Y440X}$ mutation affects the common SOXE bipartite transactivation mechanism (57), in which a transactivation domain in the middle of the protein synergizes with a C-terminal region, thereby contributing to hypomorphism/haploinsufficiency for SOX9 and/or dominant negative effects.

A similar mechanism may underlie the endolymphatic hydrops in pig *SOX10* R109W mutants with phenotypic similarities to human Mondini dysplasia (88). It is notable that a dominant negative mechanism has been proposed for the mouse $Sox10^{Dom}$ mutation that truncates SOX10 but spares the DNA binding domain (89), raising the question of to what extent the $SOX10^{Dom}$ mutation interferes with SOX9–SOX10 cooperation and impacts inner ear development.

Our findings have implications for understanding disorders affecting the ionic composition, which are the most common causes of deafness and are often associated with an enlarged vestibular aqueduct (EVA; OMIM 600791). To date, dysfunction in fluid homeostasis leading to EVA (or Pendred syndrome) has been mostly attributed to mutations in *FOXI1* (OMIM 601093) and its target gene *SLC26A4*. Our work extends the range of candidate causative mutations for common causes of dysregulated fluid homeostasis in childhood congenital deafness and also identifies disease genes regulated by the SOXE factors, which could be a guide for the diagnosis of deafness and vestibular problems (Dataset S1). Mutations of *GJB2* that encodes connexin 26, a component of the gap junction, result in deafness due to fluid imbalance (90). Our study identifies SOXE as a regulator of *Gjb2*, which is downregulated in $Sox9^{Y440X/+}$ RRCs. We also identify potential candidate EVA genes downstream of SOX9, such as genes encoding ion transporters (e.g., *Slc24a4* and *Slc15a1*), channels (*Ttyh1*), and components of the renin-angiotensin system, involved in ion transport and water regulation represented by *Agt* and *Mme*. The $Sox9^{Y440X}$ model demonstrates that having appropriate numbers of mature cells, including the *Slc26a4*+ ion transport cells, is key to ionic homeostasis and a functioning endolymphatic system.

In summary, our study reveals that depending on the target gene context, SOX9 and SOX10 act both independently and co-operatively to ensure proper development of the endolymphatic

system and ionic homeostasis (Fig. 6*G*). These functions are important both early and later in the development of the endolymphatic system and also suggest a cause of the sensorineural deafness pathology in CD. Since *SoxE* genes have many roles in embryogenesis and in adult tissue-specific stem cells, the principles we have uncovered are relevant to the effects of heterozygous dominant mutations on other cell types where SOX9 and SOX10 are coexpressed. The lessons learned from the pathogenic phenotypes that arise from disrupting transcription factors important for development are also relevant to understanding the impact of mutations in developmental transcription factors on different cells and/or tissues.

Materials and Methods

Animals. Animal care and experiments were in accordance with the protocols approved by the Committee on the Use of Live Animals in Teaching and Research of the University of Hong Kong. *Sox9*$^{Y440X/+}$ mutants were generated from a variety of crosses: floxed mutant (*Sox9*^{floxedY440X}) with the *β-actin Cre* driver (91) (provided by G. Martin, University of California, San Francisco, CA) to generate constitutive mutants. While most of these mutants died at birth, about 10% of the constitutive mutants survived. Surviving mutants were crossed to WT (C57/BL6) animals to obtain *Sox9*$^{Y440X/+}$ heterozygotes for analysis at postnatal stages. In addition, we also generated constitutive *β-actin Cre*;*Sox9*$^{Y440X/+}$ heterozygote fetuses for molecular marker analyses independently of the surviving line. Otic-specific mutant was generated by crossing the transgenic *B2-r4-Cre* mouse line (39) to *Sox9*$^{fY440X/+}$ mice to generate *B2-Sox9*$^{cY440X/+}$ and control littermates. *Sox9*$^{c/+}$ (92) mice were a gift of Andreas Schedl, Institut de Biologie Valrose, Nice, France, and Richard Behringer, MD Anderson Cancer Center, Houston, TX. SoxE compound mutants were generated by intercrossing, *Sox9*$^{cY440X/+}$, *Sox9*$^{c/+}$, and *Sox10*$^{N/+}$ (93) mice. In all cases, we compared WT and mutant littermates. All mice analyzed were of mixed genetic background. *Sox9*$^{Y440X/+}$, *Sox9*$^{c/+}$, and *Sox10*$^{N/+}$ mice were of mixed genetic background 129Sv/Ev; C57/BL6. The genetic background of *beta-actin Cre* and *B2-r4-Cre* mouse lines was Institute of Cancer Research and C57/BL6;CBA respectively (39).

SOX9^{Y440X} Antibody. The rabbit polyclonal SOX9^{Y440X} antibody was generated against the 14-aa peptide sequence before the Y440X mutation from 426 to 439, YSPSYPPITRSQYD, which was predicted to generate a neoepitope, synthesized and raised by Covalab UK Ltd. (https://www.covalab.com). Specificity of the antibody was confirmed by immunostaining on WT and *Sox9*$^{Y440X/+}$ mutant tissues (Fig. 1 *B*, *C*, and *J*).

A detailed description of other methods can be found in *SI Appendix*.

Data, Materials, and Software Availability. Sequencing data have been deposited on NCBI GEO (accession nos. GSE131196 and GSE139587) (94, 95), with the processed data interactively hosted at https://www.sbms.hku.hk/kclab/sox9-ear/ (96). Some of the bioinformatics scripts were deposited in GitHub at https://github.com/hkukclab/sox9-ear (97). All other data are included in the article and/or supporting information.

ACKNOWLEDGMENTS. We thank Gigi Wong, Becky C. M. Cheng, and Nelson W. F. Dung for technical support; Simon Chan for performing hearing and endocochlear potential tests; J.-N. Lu and Nelson W. F. Dung for assistance with single cell RNA sequencing; Calista Ng for EMSA reagents; and Reinhard Faessler, Patrick Tam, Doris Wu, Kevin Yip, Pak Sham, and Michael Zhang for helpful discussion. R.J. was supported by National Natural Science Foundation of China Grant 31771454. B.F. is supported by NIH Grant R01 AG060504. This work was supported by Research Grants Council, Hong Kong Grants HKU7222/97M (to K.S.E.C.), HKU2/02C (to K.S.E.C.), HKU4/05C (to K.S.E.C.), AoE/M-04/04 (to K.S.E.C.), and T12-708/12N (to K.S.E.C.) and the Jimmy and Emily Tang Professorship (K.S.E.C.).

Author affiliations: [a]School of Biomedical Sciences, The University of Hong Kong, Li Ka Shing Faculty of Medicine, Hong Kong, China; [b]Genome Regulation Laboratory, CAS Key Laboratory of Regenerative Biology, Joint School of Life Sciences, Guangzhou Institutes of Biomedicine and Health, Chinese Academy of Sciences, Guangzhou 510530, China; [c]Guangzhou Medical University, Guangzhou 511436, China; [d]School of Biomedical Sciences, The Chinese University of Hong Kong, Shatin, Hong Kong, China; [e]Department of Biology, College of Arts & Sciences, University of Iowa, Iowa City, IA 52242; [f]Department of Otolaryngology, College of Arts & Sciences, University of Iowa, Iowa City, IA 52242; and [g]Francis Crick Institute, London NW1 1AT, United Kingdom

[1]D.K.H.C., P.C., and K.C.C. contributed equally to this work.

[2]Present address: Department of Orthopedics and Traumatology, The University of Hong Kong –Shenzhen Hospital (HKU-SZH), Shenzhen, Guangdong 518053, China.

[3]Present address: Center for Cell Lineage and Atlas, Bioland Laboratory (Guangzhou Regenerative Medicine and Health GuangDong Laboratory), Guangzhou 510005, China.

[4]Present address: Department of Medicine, University of California, San Francisco, CA 94143.

[5]Present address: School of Biomedical Sciences, The Chinese University of Hong Kong, Shatin, Hong Kong, China.

[6]To whom correspondence may be addressed. Email: kathycheah@hku.hk.

1. V. Lefebvre, Roles and regulation of SOX transcription factors in skeletogenesis. *Curr. Top. Dev. Biol.* **133**, 171–193 (2019).
2. M. Weider, M. Wegner, SoxE factors: Transcriptional regulators of neural differentiation and nervous system development. *Semin. Cell Dev. Biol.* **63**, 35–42 (2017).
3. S. Kellerer *et al.*, Replacement of the Sox10 transcription factor by Sox8 reveals incomplete functional equivalence. *Development* **133**, 2875–2886 (2006).
4. J. C. Polanco, D. Wilhelm, T. L. Davidson, D. Knight, P. Koopman, Sox10 gain-of-function causes XX sex reversal in mice: Implications for human 22q-linked disorders of sex development. *Hum. Mol. Genet.* **19**, 506–516 (2010).
5. M. Finzsch, C. C. Stolt, P. Lommes, M. Wegner, Sox9 and Sox10 influence survival and migration of oligodendrocyte precursors in the spinal cord by regulating PDGF receptor alpha expression. *Development* **135**, 637–646 (2008).
6. Z. Y. She, W. X. Yang, Sry and SoxE genes: How they participate in mammalian sex determination and gonadal development? *Semin. Cell Dev. Biol.* **63**, 13–22 (2017).
7. C. C. Stolt, P. Lommes, R. P. Friedrich, M. Wegner, Transcription factors Sox8 and Sox10 perform non-equivalent roles during oligodendrocyte development despite functional redundancy. *Development* **131**, 2349–2358 (2004).
8. E. Suzuki *et al.*, Loss-of-function SOX10 mutation in a patient with Kallmann syndrome, hearing loss, and iris hypopigmentation. *Horm. Res. Paediatr.* **84**, 212–216 (2015).
9. V. Pingault *et al.*, Review and update of mutations causing Waardenburg syndrome. *Hum. Mutat.* **31**, 391–406 (2010).
10. J. Song *et al.*, Hearing loss in Waardenburg syndrome: A systematic review. *Clin. Genet.* **89**, 416–425 (2016).
11. S. Unger, G. Scherer, A. Superti-Furga, "Campomelic dysplasia" in *GeneReviews*, M. P. Adam *et al.*, Eds. (University of Washington, Seattle, WA, 1993), pp. 1–16.
12. J. W. Foster *et al.*, Campomelic dysplasia and autosomal sex reversal caused by mutations in an SRY-related gene. *Nature* **372**, 525–530 (1994).
13. T. Wagner *et al.*, Autosomal sex reversal and campomelic dysplasia are caused by mutations in and around the SRY-related gene SOX9. *Cell* **79**, 1111–1120 (1994).
14. D. M. Fekete, D. K. Wu, Revisiting cell fate specification in the inner ear. *Curr. Opin. Neurobiol.* **12**, 35–42 (2002).
15. S. Raft *et al.*, Ephrin-B2 governs morphogenesis of endolymphatic sac and duct epithelia in the mouse inner ear. *Dev. Biol.* **390**, 51–67 (2014).
16. P. G. Lundquist, Aspects on endolymphatic sac morphology and function. *Arch. Otorhinolaryngol.* **212**, 231–240 (1976).
17. A. N. Salt, Regulation of endolymphatic fluid volume. *Ann. N. Y. Acad. Sci.* **942**, 306–312 (2001).
18. F. Barrionuevo *et al.*, Sox9 is required for invagination of the otic placode in mice. *Dev. Biol.* **317**, 213–224 (2008).
19. A. C. Mak, I. Y. Szeto, B. Fritzsch, K. S. Cheah, Differential and overlapping expression pattern of SOX2 and SOX9 in inner ear development. *Gene Expr. Patterns* **9**, 444–453 (2009).
20. I. Breuskin *et al.*, Sox10 promotes the survival of cochlear progenitors during the establishment of the organ of Corti. *Dev. Biol.* **335**, 327–339 (2009).
21. N. Saint-Germain, Y. H. Lee, Y. Zhang, T. D. Sargent, J. P. Saint-Jeannet, Specification of the otic placode depends on Sox9 function in *Xenopus*. *Development* **131**, 1755–1763 (2004).
22. B. Y. Park, J. P. Saint-Jeannet, Long-term consequences of Sox9 depletion on inner ear development. *Dev. Dyn.* **239**, 1102–1112 (2010).
23. M. O. Trowe *et al.*, Loss of Sox9 in the periotic mesenchyme affects mesenchymal expansion and differentiation, and epithelial morphogenesis during cochlea development in the mouse. *Dev. Biol.* **342**, 51–62 (2010).
24. P. Betancur, M. Bronner-Fraser, T. Sauka-Spengler, Genomic code for Sox10 activation reveals a key regulatory enhancer for cranial neural crest. *Proc. Natl. Acad. Sci. U.S.A.* **107**, 3570–3575 (2010).
25. P. Betancur, T. Sauka-Spengler, M. Bronner, A Sox10 enhancer element common to the otic placode and neural crest is activated by tissue-specific paralogs. *Development* **138**, 3689–3698 (2011).
26. L. Kolla *et al.*, Characterization of the development of the mouse cochlear epithelium at the single cell level. *Nat. Commun.* **11**, 2389 (2020).
27. D. I. Scheffer, J. Shen, D. P. Corey, Z. Y. Chen, Gene expression by mouse inner ear hair cells during development. *J. Neurosci.* **35**, 6366–6380 (2015).
28. S. Wang, M. P. Lee, S. Jones, J. Liu, J. Waldhaus, Mapping the regulatory landscape of auditory hair cells from single-cell multi-omics data. *Genome Res.* **31**, 1885–1899 (2021).
29. W. Bi *et al.*, Haploinsufficiency of Sox9 results in defective cartilage primordia and premature skeletal mineralization. *Proc. Natl. Acad. Sci. U.S.A.* **98**, 6698–6703 (2001).
30. G. Scherer, B. Zabel, G. Nishimura, Clinical utility gene card for: Campomelic dysplasia. *Eur. J. Hum. Genet.*, 10.1038/ejhg.2012.228 (2013).
31. S. Unger, G. Scherer, A. Superti-Furga, "Campomelic dysplasia" in *GeneReviews*, R. A. Pagon, M. P. Adam, H. H. Ardinger, Eds. (University of Washington, Seattle, WA 2008), pp. 1–16.

32. R. M. Hageman, F. J. Cameron, A. H. Sinclair, Mutation analysis of the SOX9 gene in a patient with campomelic dysplasia. *Hum. Mutat.* **1** (suppl. 1), S112–S113 (1998).
33. J. Meyer *et al.*, Mutational analysis of the SOX9 gene in campomelic dysplasia and autosomal sex reversal: Lack of genotype/phenotype correlations. *Hum. Mol. Genet.* **6**, 91–98 (1997).
34. R. Pop, M. V. Zaragoza, M. Gaudette, U. Dohrmann, G. Scherer, A homozygous nonsense mutation in SOX9 in the dominant disorder campomelic dysplasia: A case of mitotic gene conversion. *Hum. Genet.* **117**, 43–53 (2005).
35. F. Csukasi *et al.*, Dominant-negative SOX9 mutations in campomelic dysplasia. *Hum. Mutat.* **40**, 2344–2352 (2019).
36. Y. H. Huang, A. Jankowski, K. S. Cheah, S. Prabhakar, R. Jauch, SOXE transcription factors form selective dimers on non-compact DNA motifs through multifaceted interactions between dimerization and high-mobility group domains. *Sci. Rep.* **5**, 10398 (2015).
37. Y. Kamachi, H. Kondoh, Sox proteins: Regulators of cell fate specification and differentiation. *Development* **140**, 4129–4144 (2013).
38. S. Sugahara, T. Fujimoto, H. Kondoh, M. Uchikawa, Nasal and otic placode specific regulation of Sox2 involves both activation by Sox-Sall4 synergism and multiple repression mechanisms. *Dev. Biol.* **433**, 61–74 (2018).
39. I. Y. Szeto, K. K. Leung, M. H. Sham, K. S. Cheah, Utility of HoxB2 enhancer-mediated Cre activity for functional studies in the developing inner ear. *Genesis* **47**, 361–365 (2009).
40. B. J. Kopecky, I. Jahan, B. Fritzsch, Correct timing of proliferation and differentiation is necessary for normal inner ear development and auditory hair cell viability. *Dev. Dyn.* **242**, 132–147 (2013).
41. V. V. Chizhikov, I. Y. Iskusnykh, N. Fattakhov, B. Fritzsch, Lmx1a and Lmx1b are redundantly required for the development of multiple components of the mammalian auditory system. *Neuroscience* **452**, 247–264 (2021).
42. S. K. Koo *et al.*, Lmx1a maintains proper neurogenic, sensory, and non-sensory domains in the mammalian inner ear. *Dev. Biol.* **333**, 14–25 (2009).
43. D. H. Nichols *et al.*, Lmx1a is required for segregation of sensory epithelia and normal ear histogenesis and morphogenesis. *Cell Tissue Res.* **334**, 339–358 (2008).
44. I. Schrauwen *et al.*, A variant in LMX1A causes autosomal recessive severe-to-profound hearing impairment. *Hum. Genet.* **137**, 471–478 (2018).
45. M. Wesdorp *et al.*; DOOFNL Consortium, Heterozygous missense variants of LMX1A lead to nonsyndromic hearing impairment and vestibular dysfunction. *Hum. Genet.* **137**, 389–400 (2018).
46. H. M. Kim, P. Wangemann, Failure of fluid absorption in the endolymphatic sac initiates cochlear enlargement that leads to deafness in mice lacking pendrin expression. *PLoS One* **5**, e14041 (2010).
47. S. Albert *et al.*, SLC26A4 gene is frequently involved in nonsyndromic hearing impairment with enlarged vestibular aqueduct in Caucasian populations. *Eur. J. Hum. Genet.* **14**, 773–779 (2006).
48. M. R. Khan, R. Bashir, S. Naz, SLC26A4 mutations in patients with moderate to severe hearing loss. *Biochem. Genet.* **51**, 514–523 (2013).
49. D. Acampora *et al.*, Craniofacial, vestibular and bone defects in mice lacking the Distal-less-related gene Dlx5. *Development* **126**, 3795–3809 (1999).
50. M. Hulander *et al.*, Lack of pendrin expression leads to deafness and expansion of the endolymphatic compartment in inner ears of Foxi1 null mutant mice. *Development* **130**, 2013–2025 (2003).
51. A. J. Griffith, P. Wangemann, Hearing loss associated with enlargement of the vestibular aqueduct: Mechanistic insights from clinical phenotypes, genotypes, and mouse models. *Hear. Res.* **281**, 11–17 (2011).
52. D. Kobak, P. Berens, The art of using t-SNE for single-cell transcriptomics. *Nat. Commun.* **10**, 5416 (2019).
53. K. Honda *et al.*, Molecular architecture underlying fluid absorption by the developing inner ear. *eLife* **6**, e26851 (2017).
54. T. A. Peters, E. L. Tonnaer, W. Kuijpers, J. H. Curfs, Changes in ultrastructural characteristics of endolymphatic sac ribosome-rich cells of the rat during development. *Hear. Res.* **176**, 94–104 (2003).
55. K. Gnedeva, A. J. Hudspeth, SoxC transcription factors are essential for the development of the inner ear. *Proc. Natl. Acad. Sci. U.S.A.* **112**, 14066–14071 (2015).
56. Y. Mao, S. Reiprich, M. Wegner, B. Fritzsch, Targeted deletion of Sox10 by Wnt1-cre defects neuronal migration and projection in the mouse inner ear. *PLoS One* **9**, e94580 (2014).
57. A. Haseeb, V. Lefebvre, The SOXE transcription factors-SOX8, SOX9 and SOX10-share a bi-partite transactivation mechanism. *Nucleic Acids Res.* **47**, 6917–6931 (2019).
58. L. Hou, Y. Srivastava, R. Jauch, Molecular basis for the genome engagement by Sox proteins. *Semin. Cell Dev. Biol.* **63**, 2–12 (2017).
59. H. Akiyama *et al.*, Interactions between Sox9 and beta-catenin control chondrocyte differentiation. *Genes Dev.* **18**, 1072–1087 (2004).
60. P. Bastide *et al.*, Sox9 regulates cell proliferation and is required for Paneth cell differentiation in the intestinal epithelium. *J. Cell Biol.* **178**, 635–648 (2007).
61. P. Bhattaram *et al.*, SOXC proteins amplify canonical WNT signaling to secure nonchondrocytic fates in skeletogenesis. *J. Cell Biol.* **207**, 657–671 (2014).
62. A. Symon, V. Harley, SOX9: A genomic view of tissue specific expression and action. *Int. J. Biochem. Cell Biol.* **87**, 18–22 (2017).
63. C. F. Liu, M. Angelozzi, A. Haseeb, V. Lefebvre, SOX9 is dispensable for the initiation of epigenetic remodeling and the activation of marker genes at the onset of chondrogenesis. *Development* **145**, dev164459 (2018).
64. S. Ohba, X. He, H. Hojo, A. P. McMahon, Distinct transcriptional programs underlie Sox9 regulation of the mammalian chondrocyte. *Cell Rep.* **12**, 229–243 (2015).
65. S. Liu, R. Guo, L. D. Quarles, Cloning and characterization of the proximal murine Phex promoter. *Endocrinology* **142**, 3987–3995 (2001).
66. C. A. Cowan, N. Yokoyama, L. M. Bianchi, M. Henkemeyer, B. Fritzsch, EphB2 guides axons at the midline and is necessary for normal vestibular function. *Neuron* **26**, 417–430 (2000).
67. A. Eckhard *et al.*, Co-localisation of K(ir)4.1 and AQP4 in rat and human cochleae reveals a gap in water channel expression at the transduction sites of endocochlear K(+) recycling routes. *Cell Tissue Res.* **350**, 27–43 (2012).
68. T. Takeda, D. Taguchi, Aquaporins as potential drug targets for Meniere's disease and its related diseases. *Handb. Exp. Pharmacol.* **190**, 171–184 (2009).
69. D. M. Bell *et al.*, SOX9 directly regulates the type-II collagen gene. *Nat. Genet.* **16**, 174–178 (1997).
70. K. A. Frazer, L. Pachter, A. Poliakov, E. M. Rubin, I. Dubchak, VISTA: Computational tools for comparative genomics. *Nucleic Acids Res.* **32**, W273-9 (2004).
71. A. Mathelier *et al.*, JASPAR 2014: An extensively expanded and updated open-access database of transcription factor binding profiles. *Nucleic Acids Res.* **42**, D142–D147 (2014).
72. A. Sandelin, W. Alkema, P. Engström, W. W. Wasserman, B. Lenhard, JASPAR: An open-access database for eukaryotic transcription factor binding profiles. *Nucleic Acids Res.* **32**, D91–D94 (2004).
73. E. Sock *et al.*, Loss of DNA-dependent dimerization of the transcription factor SOX9 as a cause for campomelic dysplasia. *Hum. Mol. Genet.* **12**, 1439–1447 (2003).
74. B. Herbarth *et al.*, Mutation of the Sry-related Sox10 gene in Dominant megacolon, a mouse model for human Hirschsprung disease. *Proc. Natl. Acad. Sci. U.S.A.* **95**, 5161–5165 (1998).
75. E. M. Southard-Smith, L. Kos, W. J. Pavan, Sox10 mutation disrupts neural crest development in Dom Hirschsprung mouse model. *Nat. Genet.* **18**, 60–64 (1998).
76. K. Dutton *et al.*, A zebrafish model for Waardenburg syndrome type IV reveals diverse roles for Sox10 in the otic vesicle. *Dis. Model. Mech.* **2**, 68–83 (2009).
77. I. Cruz-Solis *et al.*, Glutamate-dependent transcriptional control in Bergmann glia: Sox10 as a repressor. *J. Neurochem.* **109**, 899–910 (2009).
78. V. Y. Leung *et al.*, SOX9 governs differentiation stage-specific gene expression in growth plate chondrocytes via direct concomitant transactivation and repression. *PLoS Genet.* **7**, e1002356 (2011).
79. S. Schreiner *et al.*, Hypomorphic Sox10 alleles reveal novel protein functions and unravel developmental differences in glial lineages. *Development* **134**, 3271–3281 (2007).
80. M. Wahlbuhl, S. Reiprich, M. R. Vogl, M. R. Bösl, M. Wegner, Transcription factor Sox10 orchestrates activity of a neural crest-specific enhancer in the vicinity of its gene. *Nucleic Acids Res.* **40**, 88–101 (2012).
81. H. K. Long *et al.*, Loss of extreme long-range enhancers in human neural crest drives a craniofacial disorder. *Cell Stem Cell* **27**, 765–783.e14 (2020).
82. P. C. Lee *et al.*, SUMOylated SoxE factors recruit Grg4 and function as transcriptional repressors in the neural crest. *J. Cell Biol.* **198**, 799–813 (2012).
83. E. N. Schock, C. LaBonne, Sorting Sox: Diverse roles for Sox transcription factors during neural crest and craniofacial development. *Front. Physiol.* **11**, 606889 (2020).
84. K. M. Taylor, C. Labonne, SoxE factors function equivalently during neural crest and inner ear development and their activity is regulated by SUMOylation. *Dev. Cell* **9**, 593–603 (2005).
85. J. M. Hernández-Hernández *et al.*, Sox9 represses alpha-sarcoglycan gene expression in early myogenic differentiation. *J. Mol. Biol.* **394**, 1–14 (2009).
86. C. D. Pozniak *et al.*, Sox10 directs neural stem cells toward the oligodendrocyte lineage by decreasing Suppressor of Fused expression. *Proc. Natl. Acad. Sci. U.S.A.* **107**, 21795–21800 (2010).
87. S. Korrapati *et al.*, Single cell and single nucleus RNA-Seq reveal cellular heterogeneity and homeostatic regulatory networks in adult mouse stria vascularis. *Front. Mol. Neurosci.* **12**, 316 (2019).
88. T. Hai *et al.*, Pilot study of large-scale production of mutant pigs by ENU mutagenesis. *eLife* **6**, e26248 (2017).
89. V. A. Cantrell *et al.*, Interactions between Sox10 and EdnrB modulate penetrance and severity of aganglionosis in the Sox10Dom mouse model of Hirschsprung disease. *Hum. Mol. Genet.* **13**, 2289–2301 (2004).
90. J. B. Hochman *et al.*, Prevalence of Connexin 26 (GJB2) and Pendred (SLC26A4) mutations in a population of adult cochlear implant candidates. *Otol. Neurotol.* **31**, 919–922 (2010).
91. M. Lewandoski, E. N. Meyers, G. R. Martin, Analysis of Fgf8 gene function in vertebrate development. *Cold Spring Harb. Symp. Quant. Biol.* **62**, 159–168 (1997).
92. H. Akiyama, M. C. Chaboissier, J. F. Martin, A. Schedl, B. de Crombrugghe, The transcription factor Sox9 has essential roles in successive steps of the chondrocyte differentiation pathway and is required for expression of Sox5 and Sox6. *Genes Dev.* **16**, 2813–2828 (2002).
93. N. Bondurand, M. H. Sham, The role of SOX10 during enteric nervous system development. *Dev. Biol.* **382**, 330–343 (2013).
94. I. Y. Y. Szeto *et al.*, SOX9 and SOX10 control fluid homeostasis in the inner ear for hearing through independent and cooperative mechanisms (scRNA-seq: batch2). NCBI GEO. https://www.ncbi.nlm.nih.gov/geo/query/acc.cgi?acc=GSE139587. Deposited 10 October 2022.
95. I. Y. Y. Szeto *et al.*, SOX9 and SOX10 control fluid homeostasis in the inner ear for hearing through independent and cooperative mechanisms. NCBI GEO. https://www.ncbi.nlm.nih.gov/geo/query/acc.cgi?acc=GSE131196. Deposited 10 October 2022.
96. I. Y. Y. Szeto *et al.*, SOX9 and SOX10 control fluid homeostasis in the inner ear for hearing through independent and cooperative mechanisms. KC Lab Data Portal. https://www.sbms.hku.hk/kclab/sox9-ear/. Deposited 14 September 2022.
97. I. Y. Y. Szeto *et al.*, Source codes for SOX9 and SOX10 control fluid homeostasis in the inner ear for hearing through independent and cooperative mechanisms. GitHub. https://github.com/hkukclab/sox9-ear. Deposited 11 October 2022.
98. N. BabuRajendran *et al.*, Structure of Smad1 MH1/DNA complex reveals distinctive rearrangements of BMP and TGF-beta effectors. *Nucleic Acids Res.* **38**, 3477–3488 (2010).
99. S. Jerabek *et al.*, Changing POU dimerization preferences converts Oct6 into a pluripotency inducer. *EMBO Rep.* **18**, 319–333 (2017).